Innate lymphoid cells and disease tolerance in SARS-CoV-2 infection

Noah J. Silverstein[1,2,3*], Yetao Wang[1,3*], Zachary Manickas-Hill[3,4], Claudia Carbone[1], Ann Dauphin[1], Brittany P. Boribong[5,6,7], Maggie Loiselle[5], Jameson Davis[5], Maureen M. Leonard[5,6,7], Leticia Kuri-Cervantes[8,9], MGH COVID-19 Collection & Processing Team, Nuala J. Meyer[10], Michael R. Betts[8,9], Jonathan Z. Li[3,11], Bruce Walker[3,4,12,13], Xu G. Yu[3,4,11], Lael M. Yonker[5,6,7], Jeremy Luban[1,3,14,15]

[1]Program in Molecular Medicine, University of Massachusetts Medical School, Worcester, MA 01605, USA
[2]Medical Scientist Training Program, University of Massachusetts Medical School, Worcester, MA 01605, USA
[3]Massachusetts Consortium on Pathogen Readiness, Boston, MA, 02115
[4]Ragon Institute of MGH, MIT and Harvard, Cambridge, MA 02139, USA
[5]Massachusetts General Hospital, Mucosal Immunology and Biology Research Center, Boston, MA, USA
[6]Massachusetts General Hospital, Department of Pediatrics, Boston, MA, USA
[7]Harvard Medical School, Boston, MA, USA
[8]Department of Microbiology, Perelman School of Medicine, University of Pennsylvania, Philadelphia, PA 19104, USA
[9]Institute for Immunology, Perelman School of Medicine, University of Pennsylvania, Philadelphia, PA 19104, USA.
[10]Division of Pulmonary and Critical Care Medicine, Department of Medicine, University of Pennsylvania Perelman School of Medicine, Philadelphia, PA 19104, USA
[11]Department of Medicine, Brigham and Women's Hospital, Boston, MA 02115, USA
[12]Howard Hughes Medical Institute, Chevy Chase, MD 20815, USA
[13]Department of Biology and Institute of Medical Engineering and Science, Massachusetts Institute of Technology, Cambridge, MA
[14]Department of Biochemistry and Molecular Pharmacology, University of Massachusetts Medical School, Worcester, MA 01605, USA
[15]Broad Institute of Harvard and MIT, 75 Ames Street, Cambridge, MA 02142, USA

*These authors contributed equally

Correspondence: yetao.wang@umassmed.edu (Y.W.); jeremy.luban@umassmed.edu (J.L.)

Abstract:

Risk of severe COVID-19 increases with age, is greater in males, and is associated with lymphopenia, but not with higher burden of SARS-CoV-2. It is unknown whether effects of age and sex on abundance of specific lymphoid subsets explain these correlations. This study found that the abundance of innate lymphoid cells (ILCs) decreases more than 7-fold over the human lifespan — T cell subsets decrease less than 2-fold — and is lower in males than in females. After accounting for effects of age and sex, ILCs, but not T cells, were lower in adults hospitalized with COVID-19, independent of lymphopenia. Among SARS-CoV-2-infected adults, the abundance of ILCs, but not of T cells, correlated inversely with odds and duration of hospitalization, and with severity of inflammation. ILCs were also uniquely decreased in pediatric COVID-19 and the numbers of these cells did not recover during follow-up. In contrast, children with MIS-C had depletion of both ILCs and T cells, and both cell types increased during follow-up. In both pediatric COVID-19 and MIS-C, ILC abundance correlated inversely with inflammation. Blood ILC mRNA and phenotype tracked closely with ILCs from lung. Importantly, blood ILCs produced amphiregulin, a protein implicated in disease tolerance and tissue homeostasis, and the percentage of amphiregulin-producing ILCs was higher in females than in males. These results suggest that, by promoting disease tolerance, homeostatic ILCs decrease morbidity and mortality associated with SARS-CoV-2 infection, and that lower ILC abundance accounts for increased COVID-19 severity with age and in males.

INTRODUCTION

The risk of severe COVID-19 and death in people infected with SARS-CoV-2 increases with age and is greater in men than in women (Alkhouli et al., 2020; Bunders and Altfeld, 2020; Gupta et al., 2021; Laxminarayan et al., 2020; Mauvais-Jarvis, 2020; O'Driscoll et al., 2020; Peckham et al., 2020; Richardson et al., 2020; Scully et al., 2020). These trends have been observed in people infected with SARS-CoV (Chen and Subbarao, 2007; Donnelly et al., 2003; Karlberg, 2004), or with MERS-CoV (Alghamdi et al., 2014), and in laboratory animals challenged with SARS-CoV or SARS-CoV-2 (Channappanavar et al., 2017; Leist et al., 2020). Yet, the mechanisms underlying these effects of age and sex on COVID-19 morbidity and mortality remain poorly understood.

The composition and function of the human immune system changes with age and exhibits sexual dimorphism (Darboe et al., 2020; Klein and Flanagan, 2016; Márquez et al., 2020; Patin et al., 2018; Solana et al., 2012), with consequences for survival of infection, response to vaccination, and susceptibility to autoimmune disease (Flanagan et al., 2017; Giefing-Kröll et al., 2015; Márquez et al., 2020; Mauvais-Jarvis, 2020; Patin et al., 2018; Piasecka et al., 2018). Better understanding of these effects might provide clues as to why the clinical outcome of SARS-CoV-2 infection is so variable, ranging from asymptomatic to lethal (Cevik et al., 2021; He et al., 2021; Jones et al., 2021; Lee et al., 2020; Lennon et al., 2020; Ra et al., 2021; Richardson et al., 2020; Yang et al., 2021).

Survival after infection with a pathogenic virus such as SARS-CoV-2 requires not only that the immune system control and eliminate the pathogen, but that disease tolerance mechanisms limit tissue damage caused by the pathogen or by host inflammatory responses (Ayres, 2020a; McCarville and Ayres, 2018; Medzhitov et al.,

2012; Schneider and Ayres, 2008). Research with animal models has demonstrated that genetic and environmental factors can promote host fitness without directly inhibiting pathogen replication (Ayres, 2020a; Cumnock et al., 2018; Jhaveri et al., 2007; McCarville and Ayres, 2018; Medzhitov et al., 2012; Råberg et al., 2007; Sanchez et al., 2018; Schneider and Ayres, 2008; Wang et al., 2016). Although in most cases the underlying mechanism is unknown, some of these models suggest that subsets of innate lymphoid cells (ILCs) contribute to disease tolerance (Artis and Spits, 2015; Branzk et al., 2018; Califano et al., 2018; Diefenbach et al., 2020; McCarville and Ayres, 2018; Monticelli et al., 2015, 2011).

ILCs lack clonotypic antigen receptors but overlap developmentally and functionally with T cells. Based on expression of characteristic transcription factors and specific inducible cytokines, ILCs are classified into ILC1, ILC2, and ILC3 subsets that are analogous to T_H1, T_H2, and T_H17 cells respectively (Artis and Spits, 2015; Cherrier et al., 2018; Vivier et al., 2018; Yudanin et al., 2019). Additionally, some ILC subsets produce the epidermal growth factor family member amphiregulin (AREG) that maintains the integrity of epithelial barriers in the lung and intestine (Branzk et al., 2018; Jamieson et al., 2013; Monticelli et al., 2015, 2011), and promotes tissue repair (Artis and Spits, 2015; Cherrier et al., 2018; Klose and Artis, 2016; Rak et al., 2016). In models of influenza infection in mice, homeostatic ILCs and exogenous AREG promote lung epithelial integrity, decrease disease severity, and increase survival, without decreasing pathogen burden (Califano et al., 2018; Jamieson et al., 2013; Monticelli et al., 2011).

Little is known about disease tolerance in the context of human infectious diseases. Interestingly, SARS-CoV-2 viral load does not reliably discriminate

symptomatic from asymptomatic infection (Cevik et al., 2021; Jones et al., 2021; Lee et al., 2020; Lennon et al., 2021; Ra et al., 2021; Yang et al., 2021). This discrepancy between SARS-CoV-2 viral load and the severity of COVID-19 is especially pronounced in children, who rarely have severe COVID-19 (Charles Bailey et al., 2020; Li et al., 2020; Lu et al., 2020; Poline et al., 2020), though viral load may be comparable to that in adults with severe COVID-19 (Heald-Sargent et al., 2020; LoTempio et al., 2021; Yonker et al., 2020). These observations suggest that age-dependent, disease tolerance mechanisms influence the severity of COVID-19. In mice, homeostatic ILCs decrease in abundance in the lung with increasing age, and lose their ability to maintain disease tolerance during influenza infection (D'Souza et al., 2019). Although the distribution of ILCs within human tissues differs from mice and is heterogeneous among individuals (Yudanin et al., 2019), human ILCs share many features with those in mice (Vivier et al., 2018) and therefore likely perform similar roles in maintaining tissue homeostasis and disease tolerance.

ILCs in peripheral blood have been reported to be depleted in individuals with severe COVID-19 (García et al., 2020; Kuri-Cervantes et al., 2020), but it is difficult to determine the extent to which ILCs are decreased independently from the overall lymphopenia associated with COVID-19 (Chen et al., 2020; Huang et al., 2020; Huang and Pranata, 2020; Zhang et al., 2020; Zhao et al., 2020), or from the reported decreases in other blood lymphoid cell populations (Kuri-Cervantes et al., 2020; Lucas et al., 2020; Mathew et al., 2020; Mudd et al., 2020; Zheng et al., 2020). In addition, assessment of lymphoid cell abundance, in the context of a disease for which age and sex are risk factors for severity, is confounded by programmed differences in lymphocyte abundance with age and sex (Márquez et al., 2020; Patin et al., 2018). The goal of this study was to

131 determine whether the abundance of any blood lymphoid cell population was altered in
132 COVID-19, independent of age, sex, and global lymphopenia, and whether abundance of
133 any lymphoid cell population correlated with clinical outcome in SARS-CoV-2 infection.

RESULTS

Characteristics of adult blood donors hospitalized for COVID-19, treated for COVID-19 as outpatients, or SARS-CoV-2-uninfected controls

The first group of blood donors in this study included SARS-CoV-2-infected adults hospitalized for severe COVID-19 (N = 40), among whom 33 (82.5%) were admitted to the ICU, 32 (80%) required intubation with mechanical ventilation, and 7 (17.5%) died (Table 1). This group had a mean age of 57.6 (range 24 to 83) and 60% were males. The second group consisted of adults infected with SARS-CoV-2 who were treated for COVID-19 as outpatients (N=51). This group had a mean age of 36.8 years (range 23-77) and was 25.5% male (Table 1). Differences between these two SARS-CoV-2-infected groups, in terms of median age ($p = 5.2 \times 10^{-8}$) and sex ratio ($p = 3.7 \times 10^{-3}$) (Fig. 1), were consistent with the established greater risk of severe COVID-19 in older individuals and in males (Alkhouli et al., 2020; Bunders and Altfeld, 2020; Gupta et al., 2021; Laxminarayan et al., 2020; Mauvais-Jarvis, 2020; O'Driscoll et al., 2020; Peckham et al., 2020; Richardson et al., 2020; Scully et al., 2020). Available information concerning ethnicity and race of the blood donors was insufficient for statistical comparisons among the groups (Supplementary Table S1). Finally, 86 adults who donated blood prior to the SARS-CoV-2 outbreak, or who were screened at a blood donation center, were included as controls for SARS-CoV-2 infection. The age of this group spanned the range of the two groups of SARS-CoV-2-infected people (mean age 50.9; range 23 to 79), and the percentage of males (55.8%) was similar to that of the group hospitalized for COVID-19 (Table 1 and Fig. 1).

Table 1: Demographic and Clinical Characteristics of Adult Blood Donor Groups

Characteristic	Healthy Control N=86	Hospitalized N=40	Outpatient N=51
Mean age (range) - years	50.9 (23-79)	57.6 (24-83)	36.8 (23-77)
Sex – number (%)			
Male	48 (55.8)	24 (60)	13 (25.5)
Female	38 (44.2)	16 (40)	38 (74.5)
Mean symptom duration at sample collection (range) – days		21.8 (5-66)	26.9 (1-61)
ICU admission – number (%)		33 (82.5)	
Intubation with mechanical ventilation – number (%)		32 (80)	
Deaths – number (%)		7 (17.5)	
Mean time hospitalized (range) – days		34.2 (4-87)	
Max lab value – mean (range)			
CRP – mg/L		228.6 (6.5-539.5)	
ESR – mm/h		89.0 (15-146)	
D-dimer – (ng/mL)		5700 (351-11923)	

Characteristics of pediatric blood donors with COVID-19, MIS-C, or SARS-CoV-2-uninfected controls

Children are less likely than adults to have severe disease when infected with SARS-CoV-2 despite having viral loads as high as adults (Charles Bailey et al., 2020; Heald-Sargent et al., 2020; Li et al., 2020; LoTempio et al., 2021; Lu et al., 2020; Poline et al., 2020; Yonker et al., 2020). Rarely, after SARS-CoV-2 clearance from the upper airways, children can develop severe Multisystem Inflammatory Syndrome in Children (MIS-C), a life-threatening condition distinct from COVID-19 that presents with high fevers and multiorgan injury, often including coronary aneurysms, ventricular failure, or myocarditis (Cheung et al., 2020; Feldstein et al., 2021, 2020; Licciardi et al., 2020; Riphagen et al., 2020; Verdoni et al., 2020; Whittaker et al., 2020).

The first cohort of pediatric blood donors in this study consisted of patients with COVID-19 who were treated in hospital (N=11) or as outpatients (N=8). The second cohort of pediatric blood donors was patients hospitalized for MIS-C (N=11). Seventeen SARS-CoV-2-uninfected pediatric blood donors constituted a control group. No significant differences in age or percentage of males were detected among the pediatric COVID-19, MIS-C, or pediatric control groups (Supplementary Table S2 and Fig. 1).

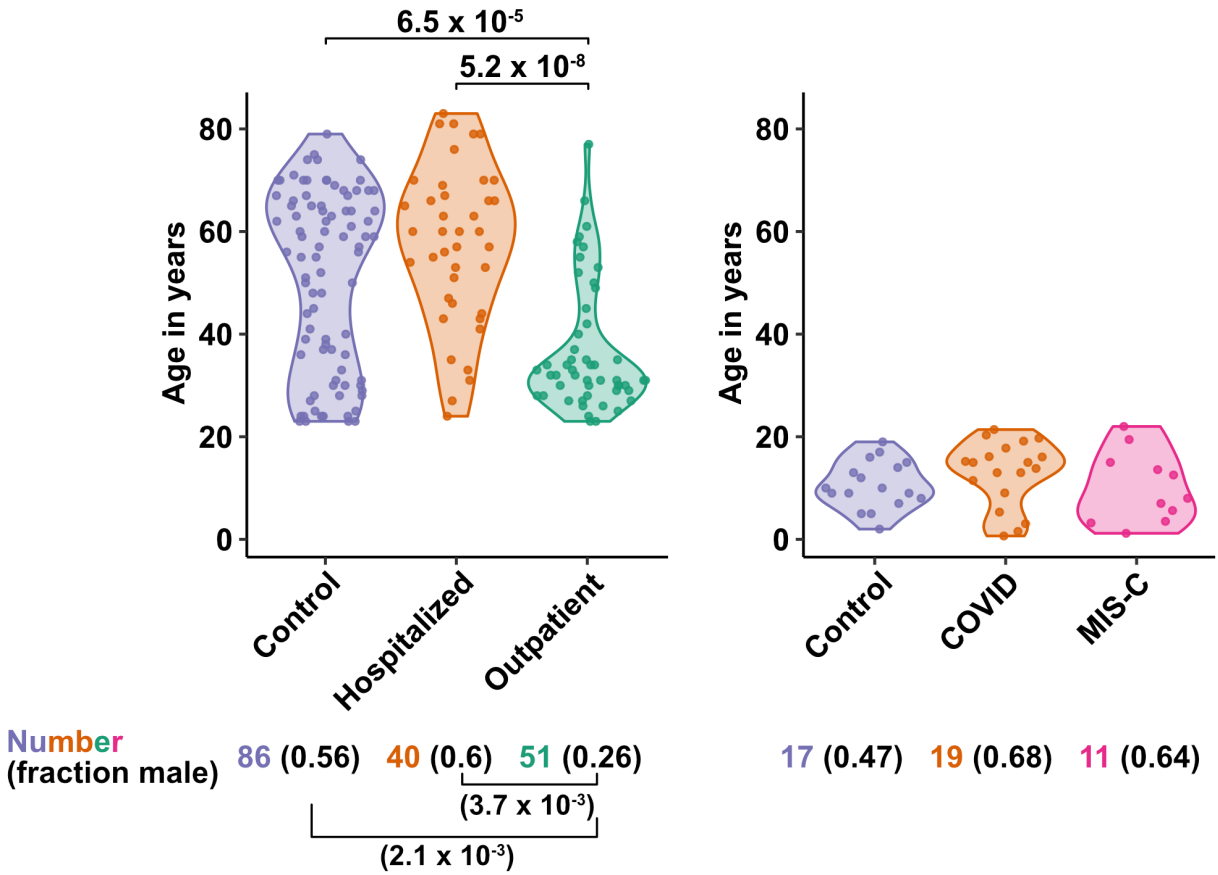

Fig. 1. Age and sex of control and SARS-CoV-2-infected blood donors

Age of the subjects is shown, along with the number of subjects and fraction male in each group, for adult (left) and pediatric (right) cohorts, as indicated. P-values are from pairwise, two-sided, Wilcoxon rank-sum test for ages and Fisher's exact test for fraction male, with Bonferroni correction for multiple comparisons. Adjusted P-values < 0.05 are shown.

Blood ILC abundance decreases exponentially across the lifespan and is sexually dimorphic

Lymphoid cell abundance in peripheral blood changes with age and is sexually dimorphic (Márquez et al., 2020; Patin et al., 2018). Previous studies reporting the effect of COVID-19 on the abundance of blood lymphoid cell subsets have not fully accounted for the association of age and sex with COVID-19 severity. To isolate the effect of COVID-19 on cell abundance from effects of age and sex, PBMCs were collected from 103 SARS-CoV-2-negative blood donors distributed from 2 to 79 years of age, with a nearly equal ratio of males to females. Abundance of lymphoid cell types was plotted by 20-year age groups (Fig. 2A), as well as by sex (Fig. 2B). Lymphoid cell types assessed here included $CD4^+$ T cells, $CD8^+$ T cells, ILCs, and FcγRIII (CD16)-positive NK cells. Like $CD8^+$ T cells, NK cells kill virus-infected cells using perforin and granzyme (Artis and Spits, 2015; Cherrier et al., 2018). Additionally, by binding virus-specific immunoglobulins that target virus-infected cells for antibody-dependent cellular cytotoxicity, $CD16^+$ NK cells link innate and acquired immunity (Anegon et al., 1988).

All cell types examined here were affected by age, but ILCs were the only subset with significant differences among all age groups, falling approximately 2-fold in median abundance every 20 years, with a greater than 7-fold decrease from the youngest to oldest age groups ($p = 1.64 \times 10^{-11}$) (Fig. 2A). This magnitude of decrease was unique to ILCs and corresponded inversely with the exponential increase in COVID-19 mortality with age (O'Driscoll et al., 2020) (Fig. 2C). In addition, both ILCs and $CD4^+$ T cells were less abundant in males (Fig. 2B). These findings highlight the importance of accounting for effects of age and sex when assessing group differences in lymphoid cell abundance,

215 particularly in the context of a disease such as COVID-19 that disproportionately affects
216 older males (O'Driscoll et al., 2020).
217

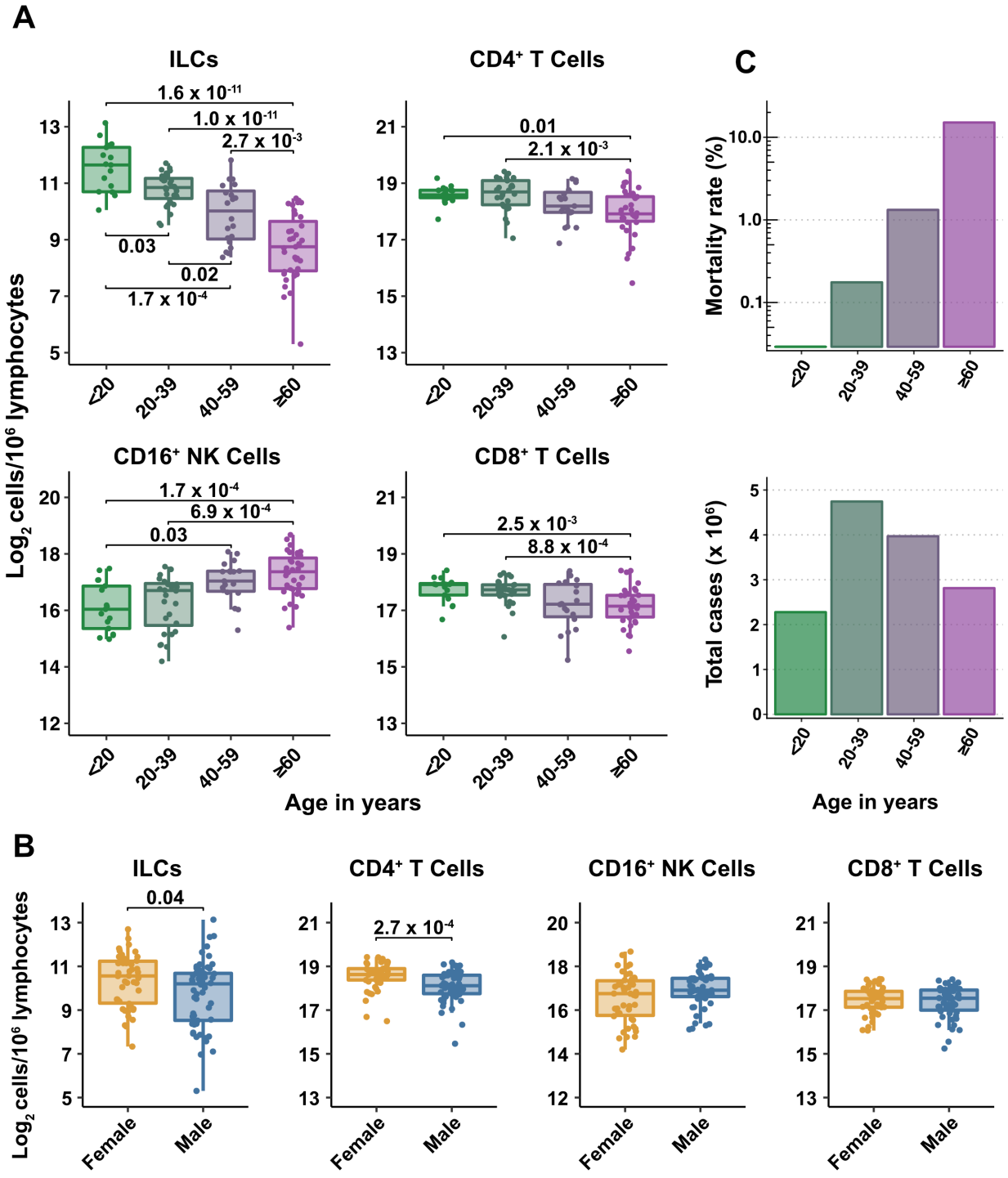

Fig. 2. Blood ILC abundance decreases exponentially across the lifespan mirroring the mortality rate from SARS-CoV-2 infection

(**A-B**) Log2 abundance per million lymphocytes of the indicated lymphoid cell populations in combined pediatric and adult control data plotted by 20-year bin or by sex, as indicated. Each dot represents an individual blood donor. Boxplots represent the distribution of the data with the center line drawn through the median with the upper and lower bounds of the box at the 75th and 25th percentiles respectively. The upper and lower whiskers extend to the largest or smallest values within 1.5 x the interquartile range (IQR). P-values are from two-sided, Wilcoxon rank-sum tests with Bonferroni correction for multiple comparisons. Adjusted P-values < 0.05 are shown.

(**C**) Case numbers and mortality rate within the indicated age ranges for cases reported in the United States between Jan 1, 2020, and June 6, 2021.

Adults hospitalized with COVID-19 have fewer total lymphocytes even after accounting for effects of age and sex

Severe COVID-19 is associated with lymphopenia (Chen et al., 2020; Huang et al., 2020; Huang and Pranata, 2020; Zhang et al., 2020; Zhao et al., 2020) but it remains unclear if this effect is due to reduction in particular lymphoid cell subpopulations, or whether this effect is explained by the more advanced age and higher proportion of males among people with severe COVID-19. As a first step to assess the specificity of lymphocyte depletion, the effect of COVID-19 on total lymphocyte abundance was addressed with multiple linear regression. After accounting for effects of age and sex, individuals hospitalized with severe COVID-19 had 1.33-fold (95%CI: 1.49–1.19; $p = 1.22 \times 10^{-6}$) fewer total lymphocytes among PBMCs than did controls (Supplementary Table S3). Lymphocyte abundance in people infected with SARS-CoV-2 who were treated as outpatients was not different from controls (Supplementary Table S3). In addition, total lymphocytes decreased with age and were less abundant in males (Supplementary Table S3). Subsequent analyses of lymphoid cell subsets took into account the depletion in total lymphocytes associated with COVID-19 by assessing lymphoid subsets as a fraction of total lymphocytes.

After accounting for age and sex, only innate lymphoid cells are depleted in severe COVID-19

To determine whether there were independent associations between lymphoid cell subsets and COVID-19, multiple linear regression was performed on the abundance of lymphoid cell subsets, with age, sex, and group (control, hospitalized, and outpatient) as independent variables. Across all three groups of adult blood donors, $CD4^+$ T cells, $CD8^+$

267 T cells, and ILCs decreased with age, while CD16$^+$ NK cells increased with age, and both
268 CD4$^+$ T cells and ILCs were less abundant in males (Table 2 and Fig. 3A).
269

Table 2: Change in Cell Abundance Due to Age, Sex, and COVID-19 Severity

Fold difference (log2) [±95%CI]

	CD4$^+$ T^a	**ILC^a**	**CD8$^+$ T^a**	**CD16$^+$ NK^a**
Age	-0.012***	-0.043***	-0.009*	0.021***
	[-0.018, -0.005]	[-0.053, -0.033]	[-0.016, -0.002]	[0.010, 0.032]
Male	-0.409***	-0.334*	-0.177	0.184
	[-0.618, -0.201]	[-0.659, -0.010]	[-0.406, 0.051]	[-0.169, 0.538]
Hospitalized	0.168	-0.835***	0.227	-1.205***
	[-0.084, 0.421]	[-1.228, -0.441]	[-0.050, 0.503]	[-1.633, -0.778]
Outpatient	0.332*	-0.088	-0.023	-0.522*
	[0.082, 0.581]	[-0.478, 0.302]	[-0.298, 0.253]	[-0.948, -0.095]
R^2	0.275	0.478	0.070	0.232

* $p < 0.05$, ** $p < 0.01$, *** $p < 0.001$
[a] per 10^6 lymphocytes
270

271 When effects of age and sex were held constant, adults hospitalized with COVID-
272 19 had 1.78-fold fewer ILCs (95%CI: 2.34–1.36; $p = 4.55 \times 10^{-5}$) and 2.31-fold fewer
273 CD16$^+$ natural killer (NK) cells (95%CI: 3.1–1.71; $p = 1.04 \times 10^{-7}$), as compared to controls
274 (Table 2 and Fig. 3B). Similar effects were also seen with ILC precursors (ILCP)
275 (Supplementary Fig. S1). Neither CD4$^+$ T cells nor CD8$^+$ T cells were depleted further
276 than expected for age and sex (Table 2 and Fig. 3B). As compared with controls, SARS-
277 CoV-2-infected adults with less severe COVID-19 who were treated as outpatients had

no reduction in ILCs, but 1.44-fold fewer $CD16^+$ NK cells (95%CI: 1.93–1.07; p = 0.018), and 1.26-fold higher $CD4^+$ T cells (95%CI: 1.06–1.5; $p = 9.59 \times 10^{-3}$) (Table 2 and Fig. 3B). As these analyses were performed on lymphoid cell abundance normalized to total lymphocyte number, it is possible that T cells were not lower in patients hospitalized with COVID-19 because the amount of depletion was not in excess of the change in total lymphocytes. However, the cell-type specific results remained unchanged even when the analyses were repeated using the less stringent threshold of normalizing to total PBMC number (Supplementary Table S4).

When data from an independent, previously published cohort (Kuri-Cervantes et al., 2020) were analyzed to account for total lymphocyte abundance, age, and sex, people hospitalized with acute respiratory distress syndrome due to COVID-19, had 1.7-fold fewer ILCs (95%CI: 2.38–1.22; p = 0.002) than controls (Supplementary Fig. S2). Also consistent with the main adult cohort studied here, ILC abundance was not significantly reduced in the group of patients with less severe disease (Supplementary Fig. S2).

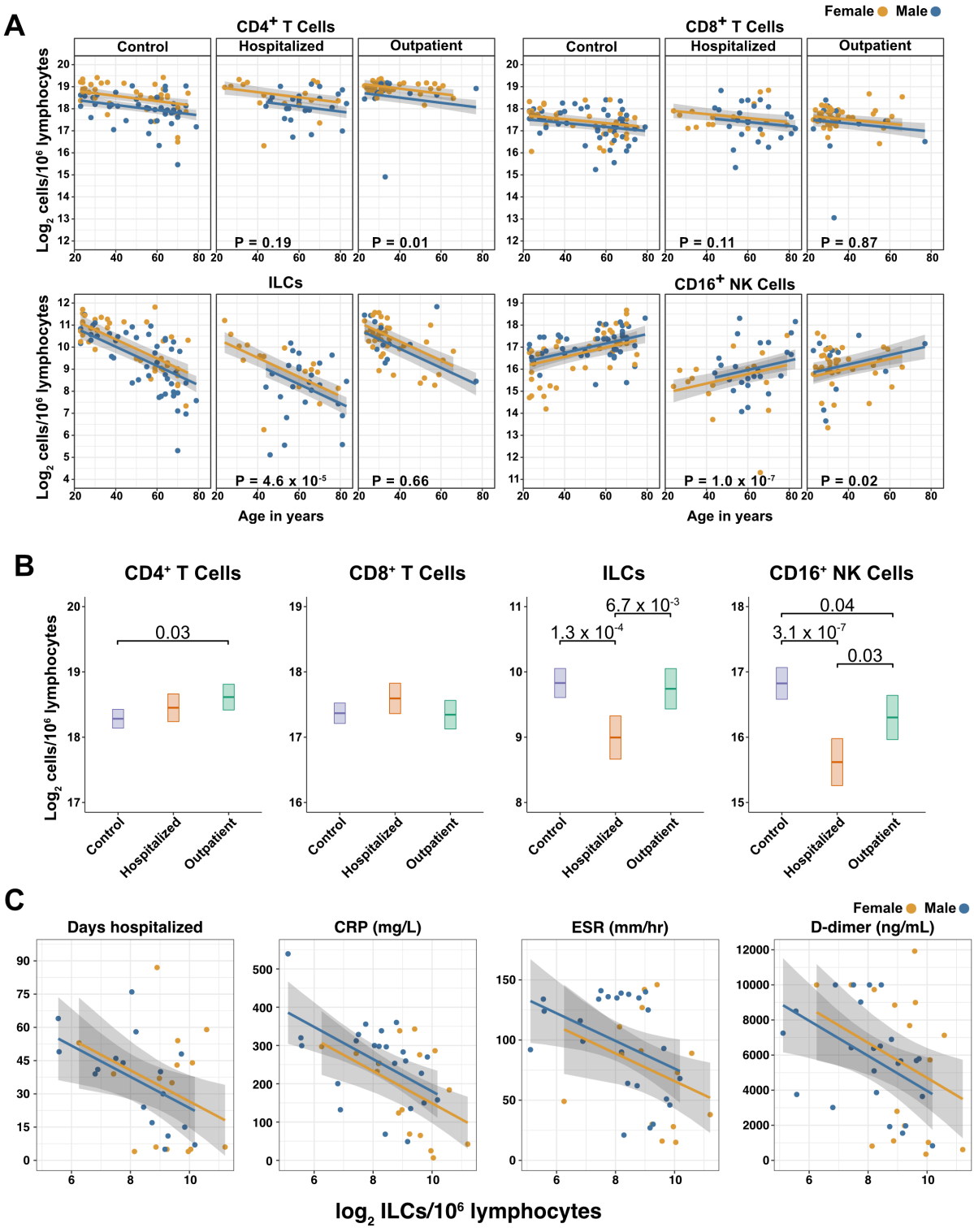

Fig. 3. Innate lymphoid cells are depleted in adults hospitalized with COVID-19 and ILC abundance correlates inversely with disease severity.

(**A**) Effect of age (X-axis) on log2 abundance per million total lymphocytes of the indicated lymphoid cell populations (Y-axis), as determined by the regression analysis in Table 2. Each dot represents an individual blood donor, with yellow for female and blue for male. Shading represents the 95%CI. P-values are from the regression analysis for comparisons to the control group.

(**B**) Log2 abundance per million lymphocytes of the indicated lymphoid cell populations, shown as estimated marginal means with 95%CI, generated from the multiple linear regressions in Table 2, and averaged across age and sex. P-values represent pairwise comparisons on the estimated marginal means, adjusted for multiple comparisons with the Tukey method. Adjusted P-values < 0.05 are shown.

(**C**) Association of the indicated clinical parameters with log2 abundance of ILCs per million lymphoid cells. Regression lines are from simplified multiple regression models to permit visualization on a two-dimensional plane. Shading represents the 95%CI. Results of the full models accounting for effects of both age and sex, are reported in Table 4 and the text.

Odds of hospitalization in adults infected with SARS-CoV-2 increases with decreasing number of ILCs

Multiple logistic regression was used next to determine whether differences in abundance of any lymphoid cell subset was associated with odds of hospitalization in people infected with SARS-CoV-2. The adjusted odds ratio was calculated using lymphoid cell subset abundance, age, sex, and duration of symptoms at the time of blood draw, each as independent variables. Abundance of ILCs, but not of $CD16^+$ NK cells, $CD4^+$ T cells, or $CD8^+$ T cells was associated with odds of hospitalization: the odds ratio for hospitalization, adjusted for age, sex, and symptom duration, was 0.413 (95%CI: 0.197–0.724; p = 0.00691), an increase of 58.7% for each 2-fold decrease in ILC abundance (Table 3).

Table 3: Odds of Hospitalization[a]

Cell count[b]	Odds Ratio[c]	95% Confidence Interval	P-Value
$CD4^+$ T	0.501	0.184–1.07	0.106
ILC	0.413	0.197–0.724	0.007
$CD8^+$ T	1.22	0.635–2.64	0.579
$CD16^+$ NK	0.814	0.53–1.21	0.309

[a]Adjusted for age, sex, and symptom duration at time of sample collection
[b]per 10^6 lymphocytes
[c]per 2-fold increase in cell population abundance

Duration of hospital stay in adults with COVID-19 increases with decreasing ILC abundance

The relationship between lymphoid cell abundance and duration of hospitalization was assessed to determine whether the association between ILC abundance and COVID-19

334 severity extended to clinical outcomes within the hospitalized adults. This relationship
335 was assessed with multiple linear regression, including age, sex, and cell abundance as
336 independent variables. Holding age and sex constant, abundance of ILCs, but not of
337 $CD16^+$ NK cells, $CD4^+$ T cells, or $CD8^+$ T cells, was associated with length of time in the
338 hospital: each two-fold decrease in ILC abundance was associated with a 9.38 day
339 increase in duration of hospital stay (95% CI: 15.76–3.01; p = 0.0054) (Fig. 3C and Table
340 4).

Table 4: Association of cell type abundance with time in hospital and laboratory values[a]

Cell count[b]	Days hospitalized	CRP (mg/L)[c]	ESR (mm/h)[c]	D-dimer (ng/mL)[c]
$CD4^+$ T	-10.843	-3.335	-2.674	-1868.847*
	[-22.511, 0.825]	[-56.162, 49.492]	[-23.840, 18.492]	[-3375.630, -362.063]
ILC	-9.381**	-46.288***	-11.035*	-1098.515*
	[-15.755, -3.008]	[-71.337, -21.238]	[-21.936, -0.134]	[-1932.842, -264.188]
$CD8^+$ T	3.366	32.247	15.317	486.192
	[-8.992, 15.724]	[-16.509, 81.003]	[-4.127, 34.761]	[-1049.836, 2022.221]
$CD16^+$ NK	-4.775	-14.619	-5.159	-404.873
	[-11.251, 1.701]	[-44.011, 14.774]	[-16.809, 6.491]	[-1316.261, 506.516]

* $p < 0.05$, ** $p < 0.01$, *** $p < 0.001$
[a]coefficients are for each two-fold increase in cell population abundance, adjusted for age and sex [±95%CI]
[b]per 10^6 lymphoid cells
[c]Maximum lab value recorded during course of hospitalization

341 **ILC abundance correlates inversely with markers of inflammation in adults**
342 **hospitalized with COVID-19**

343 To further characterize the extent to which lymphoid cell abundance predicted COVID-19

severity, multiple regression with age, sex, and cell abundance, as independent variables, was performed on peak blood levels of inflammation markers indicative of COVID-19 severity: C-reactive protein (CRP) and erythrocyte sedimentation rate (ESR), and the fibrin degradation product D-dimer (Gallo Marin et al., 2020; Gupta et al., 2021; Luo et al., 2020; Zhang et al., 2020; Zhou et al., 2020). Holding age and sex constant, each two-fold decrease in ILC, but not in $CD16^+$ NK cell, $CD4^+$ T cell, or $CD8^+$ T cell abundance, was associated with a 46.29 mg/L increase in blood CRP (95% CI: 71.34–21.24; $p = 6.25 \times 10^{-4}$) and 11.04 mm/h increase in ESR (95% CI: 21.94–0.13; $p = 0.047$) (Fig. 3C and Table 4). Abundance of both ILCs and $CD4^+$ T cells was associated with blood levels of D-dimer, with each two-fold decrease in cell abundance associated with an increase in D-dimer by 1098.52 ng/mL (95% CI: 1932.84–264.19; $p = 0.011$) and 1868.85 ng/mL (95% CI: 3375.63–362.06; $p = 0.016$), respectively (Table 4).

ILCs are depleted in children and young adults with COVID-19 or MIS-C

Given the decline in ILC abundance with age (Fig.s 2A and 3A, and Table 2), and the inverse relationship between ILC abundance and disease severity in adults (Fig. 3C, Table 3, and Table 4), it was hypothesized that children as a group have less severe COVID-19 because ILC abundance is higher at younger ages, and that pediatric cases with symptomatic SARS-CoV-2 infection, or with MIS-C, are accompanied by significantly lower numbers of ILCs. To test these hypotheses, the abundance of lymphoid cell subsets in pediatric COVID-19 or MIS-C was compared with that from pediatric controls, using multiple linear regression with age, sex, and group as independent variables. Consistent with the findings in adults, blood ILCs in the pediatric cohort decreased with age (Table 5 and Fig. 4A), demonstrating that the decrease in ILC abundance across the lifespan is

already evident within the first two decades of life. In contrast, significant change over this age range was not detected in the abundance of $CD4^+$ T cells, $CD8^+$ T cells, or $CD16^+$ NK cells (Table 5 and Fig 4A).

Among pediatric patients with COVID-19, no difference in abundance of the lymphoid cell subsets was associated with hospitalization (Supplementary Table S5), so all pediatric patients treated for COVID-19 were analyzed as a single group. After accounting for effects of age and sex, pediatric patients with COVID-19 had 1.69-fold fewer ILCs (95%CI: 2.73–1.04; p = 0.034) than controls (Fig 4A and Table 5). Neither $CD4^+$ T cells, $CD8^+$ T cells, nor $CD16^+$ NK cells were depleted in pediatric COVID-19 patients (Fig 4A and Table 5).

As with pediatric COVID-19, ILCs were also lower in MIS-C, with 2.14-fold fewer ILCs (95%CI: 3.69–1.24; p = 0.007) than controls (Fig. 4A and Table 5). However, unlike pediatric COVID-19, individuals with MIS-C had reduced numbers of T cells as compared with pediatric controls, with 1.6-fold fewer $CD4^+$ T cells (95%CI: 2.04–1.26; $p = 3.28x10^{-4}$) and 1.42-fold fewer $CD8^+$ T cells (95%CI: 1.87–1.07; p = 0.016) (Fig. 4A and Table 5). Depletion of T cells, then, distinguished MIS-C from both pediatric and adult COVID-19. Additionally, consistent with the finding in adults hospitalized with COVID-19 (Fig. 3C and Table 4), after accounting for effect of group, each two-fold decrease in ILC abundance in pediatric patients hospitalized with COVID-19 or MIS-C was associated with a 40.5 mg/L increase in blood CRP (95% CI: 77.87–3.13; p = 0.035) (Fig. 4C), and no such association was detected with $CD4^+$ T cells, $CD8^+$ T cells, or CD16+ NK cells.

Table 5: Change in Pediatric Cohort Cell Abundance Due to Age, Sex, and Group

Fold difference (log2) [±95%CI]

	CD4⁺ T[a]	ILC[a]	CD8⁺ T[a]	CD16⁺ NK[a]
Age	-0.004	-0.083**	0.012	0.004
	[-0.027, 0.019]	[-0.135, -0.032]	[-0.014, 0.039]	[-0.060, 0.068]
Male	-0.219	-0.027	0.060	-0.343
	[-0.492, 0.054]	[-0.640, 0.586]	[-0.249, 0.370]	[-1.098, 0.413]
COVID	0.018	-0.754*	-0.088	0.416
	[-0.290, 0.327]	[-1.447, -0.061]	[-0.432, 0.257]	[-0.424, 1.257]
MIS-C	-0.678***	-1.098**	-0.503*	-0.498
	[-1.028, -0.328]	[-1.884, -0.313]	[-0.904, -0.101]	[-1.479, 0.483]
R^2	0.359	0.342	0.169	0.106

* p < 0.05, ** p < 0.01, *** p < 0.001

[a]per 10^6 lymphocytes

The above analysis of lymphoid cell subsets in pediatric COVID-19 and MIS-C was performed in comparison to pediatric controls alone. Results were essentially unchanged when multiple linear regression was repeated with combined pediatric and adult control groups (Fig. 4B, Supplementary Fig. S3, and Supplementary Table S6).

Pediatric MIS-C is distinguished from COVID-19 by recovery of ILCs during follow-up

The availability of follow-up samples in this pediatric cohort provided the opportunity to assess the abundance of lymphoid subsets after recovery from illness. To this end, a linear mixed model was fit to determine the change in ILC abundance from acute illness

to follow-up in 10 individuals (5 COVID-19 and 5 MIS-C) for whom both acute and follow-up samples were available. After accounting for effects of age, sex, and group, individuals recovering from MIS-C had a 2.39-fold increase in ILC abundance (95%CI: 1.49–3.81; p = $6.6x10^{-3}$) but there was no significant change in ILC abundance for individuals recovering from COVID-19 (Fig. 4D). Both $CD4^+$ and $CD8^+$ T cells, which were depleted in MIS-C but not in COVID-19, also increased during recovery from MIS-C and remained unchanged during recovery from COVID-19 (Supplementary Fig. S4).

The relationship between time to follow-up and lymphoid cell abundance was then examined for all available follow-up samples whether or not a paired sample from the acute illness was available (COVID-19, N=14; MIS-C, N=7). This analysis found no relationship between time to follow-up and abundance of any lymphoid subset, and that individuals recovering from MIS-C had 2.28-fold more ILCs (95%CI: 1.11–4.69; p = 0.0265) than individuals recovering from COVID-19 (Fig. 4E). There was no difference between the follow-up groups in $CD4^+$ T cells, $CD8^+$ T cells, or $CD16^+$ NK cells (Fig. 4E). Interestingly, prior to being hospitalized with MIS-C, only one of these patients had COVID-19 symptoms and, despite low ILC abundance in the COVID-19 follow-up cohort, only 28.6% of this group had been ill enough to require hospitalization (Supplementary Table S2).

Differences between COVID-19 and MIS-C in regards to T cell depletion and ILC recovery during follow-up indicate that the underlying processes causing lower ILC abundance in these two SARS-CoV-2-associated diseases are different.

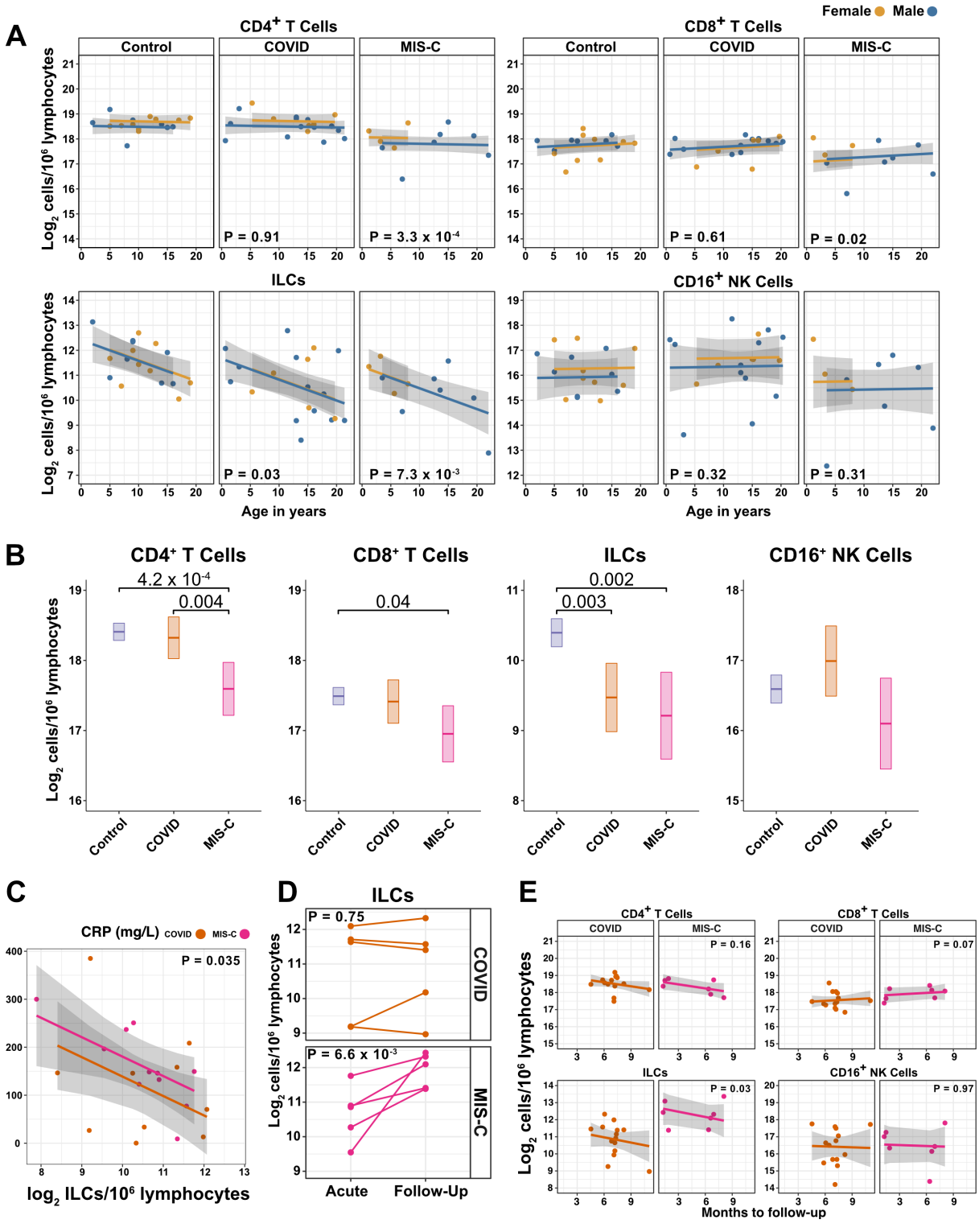

Fig. 4. ILCs are depleted in children with COVID-19 or MIS-C

(**A**) Effect of age (X-axis) on log2 abundance per million lymphocytes of the indicated lymphoid cell populations (Y-axis), as determined by the regression analysis in Table 5. Each dot represents an individual blood donor, with yellow for female and blue for male. Shading represents the 95%CI. P-values are from the regression analysis for comparisons to the control group.

(**B**) Log2 abundance per million lymphocytes of the indicated lymphoid cell populations, shown as estimated marginal means with 95%CI, generated from the multiple linear regressions in Table S6 that included the combined pediatric and adult control data, and averaged across age and sex. P-values represent pairwise comparisons on the estimated marginal means, adjusted for multiple comparisons with the Tukey method. Adjusted P-values < 0.05 are shown.

(**C**) Association of CRP with log2 abundance of ILCs per million lymphocytes. Shading represents the 95%CI. Each dot represents a single blood donor, orange for COVID-19, magenta for MIS-C. P-value is for the effect of ILC abundance on CRP as determined by linear regression.

(**D**) Log2 ILC abundance per million lymphocytes in longitudinal pairs of samples collected during acute presentation and during follow-up, from individual children with COVID-19 or MIS-C. Each pair of dots connected by a line represents an individual blood donor. P-values are for change in ILC abundance at follow-up, as determined with a linear mixed model, adjusting for age, sex, and group, and with patient as a random effect.

(**E**) Effect of time to follow-up (X-axis) on log2 abundance per million lymphocytes of the indicated lymphoid cell populations (Y-axis). P-values are for the difference between the

446 COVID-19 and MIS-C follow-up groups, independent of time to follow-up as determined
447 by linear regression. Shading represents the 95%CI.

448 **Blood ILCs resemble homeostatic ILCs isolated from lung**

449 In response to the observations described above regarding abundance of blood ILCs and
450 severity of COVID-19 attempts were made to extend these studies to lung ILCs. It was
451 not possible to obtain lung samples from people with COVID-19. However, ILCs circulate
452 from tissues to the bloodstream in lymphatic drainage via the thoracic duct suggesting
453 that measurement of blood ILCs could provide a surrogate for assessment of tissue-
454 resident ILCs, including those from the lung. Furthermore, reduction in blood ILCs in
455 people living with HIV-1 infection is paralleled by decreased ILC numbers within the
456 lamina propria of the colon (Wang et al., 2020), and so the lower abundance of blood
457 ILCs associated with severe COVID-19 might be paralleled by decreased abundance of
458 homeostatic ILCs in the lung.

459 Given the inability to assess lung samples from people with COVID-19, RNA
460 sequencing (RNA-Seq) was performed on blood ILCs from nine healthy controls and
461 these data were compared to previously published RNA-Seq profiles of ILCs sorted from
462 lung, spleen, and intestine (Ardain et al., 2019; Yudanin et al., 2019). Unbiased principal
463 component analysis demonstrated overlap of blood ILCs with lung ILCs and clear
464 separation from ILCs of jejunum or spleen (Fig. 5A). 355 genes were consistently
465 differentially expressed (fold-change > 1.5, padj < 0.01) when either blood or lung ILCs
466 were compared to ILCs from the other tissues (Fig. 5B,C). Gene ontology analysis
467 demonstrated enrichment for terms associated with type 2 immunity (Supplementary
468 Table S7). Genes significantly higher in both blood and lung ILCs included the ILC2-

469 defining genes GATA3 and PTGDR2 (CRTH2), as well as other genes important for ILC
470 development such as TCF7 (Yang et al., 2013) (Fig. 5B,C). As confirmation of the RNA
471 signature, TCF7- and CRTH2-encoded proteins were detected in blood ILCs by flow
472 cytometry (Fig. 6A).

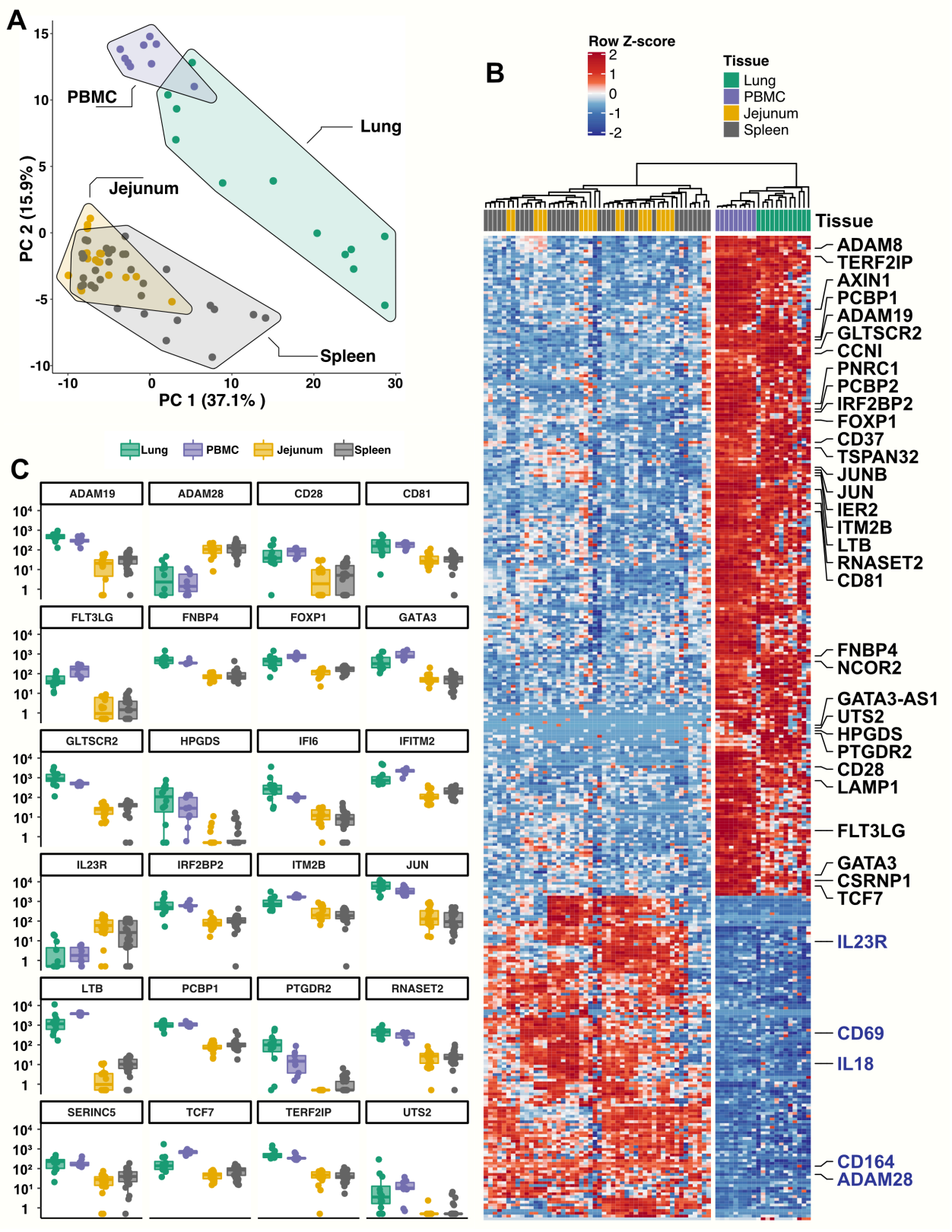

Fig. 5. Blood ILCs are transcriptionally similar to lung ILCs

RNA-seq of ILCs sorted from blood of 9 SARS-CoV-2-uninfected controls in comparison to RNA-seq data of ILCs sorted from jejunum, lung, and spleen.

(**A**) PCA plot of first two principal components calculated from the top 250 most variable genes across all samples. Each dot represents an individual sample with blue for ILCs sorted from blood, green for lung, yellow for jejunum, and grey for spleen.

(**B**) Heatmap of 355 genes differentially expressed (fold-change > 1.5, padj < 0.01 as determined with DESeq2) between either blood or lung ILCs and ILCs from the other tissues.

(**C**) Select genes from (B) plotted as deseq2 normalized counts. Each dot represents an individual sample with blue for ILCs sorted from blood, green for lung, yellow for jejunum, and grey for spleen. Boxplots represent the distribution of the data with the center line drawn through the median with the upper and lower bounds of the box at the 75th and 25th percentiles respectively. The upper and lower whiskers extend to the largest or smallest values within 1.5 x the interquartile range (IQR).

Blood ILCs are functional ILC2s capable of producing AREG

To assess the function of blood ILCs, PBMCs were stimulated with PMA and ionomycin, and assayed by flow cytometry for production of IL-13 after intracellular cytokine staining and gating on ILCs. IL-13 was detected in the stimulated ILC population (Fig. 6B), demonstrating that the majority of blood ILCs function as ILC2s. Additionally, the blood ILCs produced amphiregulin (Fig. 6B), a protein implicated in the promotion of disease tolerance by ILCs in animal models (Branzk et al., 2018; Diefenbach et al., 2020; Jamieson et al., 2013; McCarville and Ayres, 2018; Monticelli et al., 2015, 2011).

Females have a higher fraction of amphiregulin-producing blood ILCs than do males

Given the role AREG-producing ILCs play in maintaining disease tolerance in animal models (Branzk et al., 2018; Diefenbach et al., 2020; McCarville and Ayres, 2018; Monticelli et al., 2015, 2011), sex differences in the functional capability of these ILCs could contribute to the greater risk for severe COVID-19 in males (O'Driscoll et al., 2020). To address this hypothesis, ILCs isolated from peripheral blood of controls were stimulated with PMA and ionomycin, and assayed by flow cytometry for AREG production. Consistent with the apparently lower disease tolerance in males, males had a lower median fraction of $AREG^+$ ILCs than did females (P=0.018) (Fig. 6C). This difference was also reflected in a significantly lower AREG Mean Fluorescent Intensity (MFI) in males, and neither fraction of $AREG^+$ ILCs nor AREG MFI was affected by age (Supplementary Fig. S5).

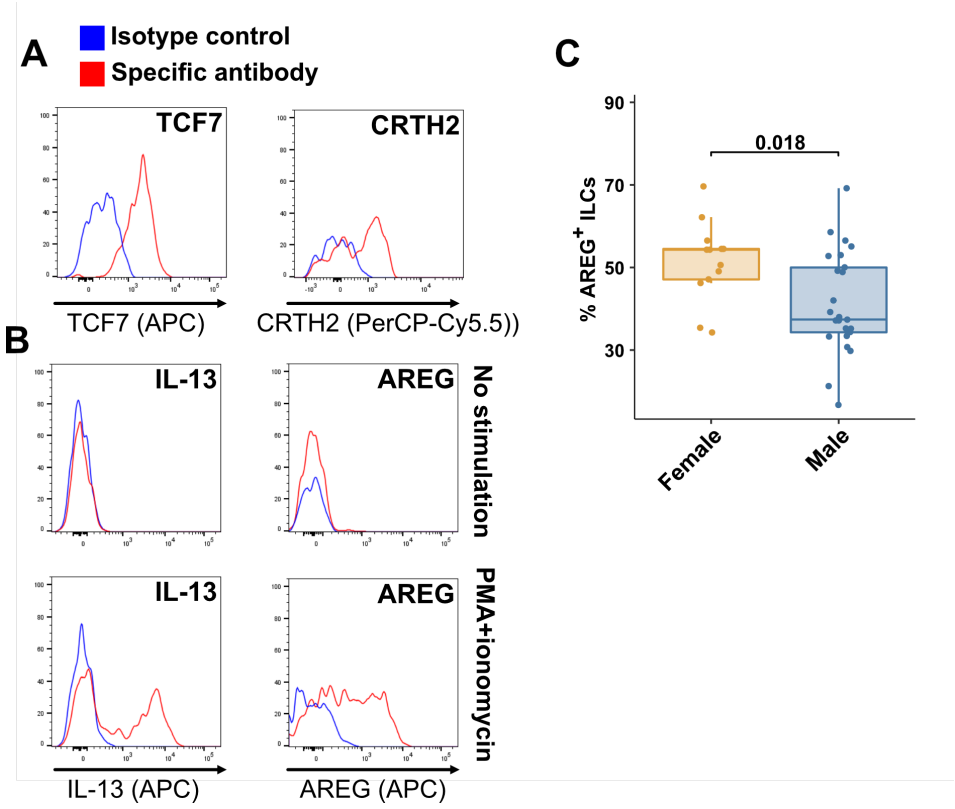

Fig. 6. Peripheral blood ILCs exhibit homeostatic ILC2 functions

(**A-B**) Flow cytometry for the indicated proteins. Cells in (A) were assayed at steady-state and cells in (B) were assayed either at steady-state or after stimulation with PMA and ionomycin, as indicated. Detection of surface proteins was performed on ILCs gated as $Lin^{-}CD56^{-}CD127^{+}$ and detection of intracellular proteins was performed on ILCs gated as $Lin^{-}TBX21^{-}CD127^{+}$.

(**C**) Percent of $AREG^{+}$ ILCs in blood of control blood donors after stimulation with PMA and ionomycin. Each dot represents an individual blood donor. Boxplots represent the distribution of the data with the center line drawn through the median with the upper and lower bounds of the box at the 75th and 25th percentiles respectively. The upper and lower whiskers extend to the largest or smallest values within 1.5 x the interquartile range (IQR). P-value is from a two-sided, Wilcoxon rank-sum test.

DISCUSSION

The outcome of SARS-CoV-2 infection ranges from entirely asymptomatic to lethal COVID-19 (Cevik et al., 2021; He et al., 2021; Jones et al., 2021; Lee et al., 2020; Lennon et al., 2020; Ra et al., 2021; Richardson et al., 2020; Yang et al., 2021). Yet, viral load does not reliably discriminate asymptomatic from symptomatic or hospitalized populations (Cevik et al., 2021; Jones et al., 2021; Lee et al., 2020; Lennon et al., 2020; Ra et al., 2021; Yang et al., 2021). In contrast, demographic factors, including increasing age and male sex, predict worse outcome of SARS-CoV-2 infection (Alkhouli et al., 2020; Bunders and Altfeld, 2020; Gupta et al., 2021; Laxminarayan et al., 2020; Mauvais-Jarvis, 2020; O'Driscoll et al., 2020; Peckham et al., 2020; Richardson et al., 2020; Scully et al., 2020). These demographic risk factors could be due to sexual dimorphism and changes with aging in composition and function of the human immune system (Darboe et al., 2020; Klein and Flanagan, 2016; Márquez et al., 2020; Patin et al., 2018; Solana et al., 2012). Therefore it is necessary to account for effects of age and sex to determine if there are additional, independent, effects of SARS-CoV-2-associated disease.

This study collected and analyzed 245 blood samples from 177 adult and 58 pediatric patients and controls, spanning the ages of 0.7 to 83 years, with approximately equal numbers of males and females. It was therefore possible to characterize the independent effects of age, sex, COVID-19, and MIS-C on blood lymphoid cell populations. After accounting for effects of age and sex, ILCs, but not $CD4^+$ or $CD8^+$ T cells, were lower in individuals hospitalized with COVID-19 when compared with controls (Table 2 and Fig. 3A,B). Lower numbers of ILCs were also observed in children with COVID-19 (Table 5 and Fig. 4A,B), as well as in an independent cohort of adult patients

(Supplementary Fig. S2). Among adults infected with SARS-CoV-2, lower abundance of ILCs, but not of the other lymphoid cell subsets, was associated with increased odds of hospitalization, longer duration of hospitalization, and higher blood level of factors associated with systemic inflammation, including CRP (Tables 3 and 4, and Fig. 3C). This inverse relationship between ILC abundance and CRP was also evident in children with COVID-19 or MIS-C (Fig. 4C).

The identification of reduced ILC numbers as uniquely related to COVID-19 severity is important as these cells mediate disease tolerance in animal models (Artis and Spits, 2015; Branzk et al., 2018; Califano et al., 2018; Diefenbach et al., 2020; McCarville and Ayres, 2018; Monticelli et al., 2015, 2011). The results here therefore indicate that loss of ILCs from blood correlates with loss of ILC-associated homeostatic functions, thereby allowing more severe COVID-19. Although this study examined circulating blood lymphoid cells, and does not provide direct information about processes occurring within tissues, transcriptional and functional characterization of blood ILCs demonstrated that these cells are similar to ILCs isolated from lung tissue (Fig. 5). Human ILCs circulate in lymphatic fluid draining from the tissues to the blood via the thoracic duct, raising the possibility that some ILCs in the blood originate from, or traffic to, lung tissue. Further characterization of these blood ILCs showed that they are functional ILC2s capable of producing the protein AREG (Fig. 6A,B). Given the tissue homeostatic role AREG plays in animal models of disease tolerance (Branzk et al., 2018; Diefenbach et al., 2020; Jamieson et al., 2013; McCarville and Ayres, 2018; Monticelli et al., 2015, 2011), the discovery here that males have a smaller fraction than females of blood ILCs capable of producing AREG (Fig. 6C) could explain why males are at greater risk of death from

SARS-CoV-2 infection (O'Driscoll et al., 2020). This sexual dimorphism in ILC function would be amplified further by the lower overall abundance of ILCs in males (Fig. 2B and Table 3).

Although the inverse relationship between the number of blood ILCs and severity of COVID-19 suggests that loss of ILC homeostatic function results in breakdown of disease tolerance (Arpaia et al., 2015; Artis and Spits, 2015; Branzk et al., 2018; Diefenbach et al., 2020; McCarville and Ayres, 2018; Monticelli et al., 2015, 2011), this observational study cannot determine whether ILC depletion preceded SARS-CoV-2 infection or whether ILC numbers are depleted as a consequence of SARS-CoV-2 infection. However, several observations support the hypothesis that individuals with lower ILC numbers at the time of SARS-CoV-2 infection are at greater risk of developing severe disease. ILC numbers in uninfected controls decrease exponentially with age; this decrease is much larger than that seen with other lymphoid cell types (Fig. 2A), and much more closely mirrors the exponential increase in COVID-19 mortality with age (O'Driscoll et al., 2020) (Fig. 2C). In addition, the greater risk of COVID-19 mortality in males (O'Driscoll et al., 2020) correlates with lower abundance of blood ILCs (Fig. 2B and Table 3) and smaller fraction of ILCs capable of producing AREG (Fig. 6C). Further supporting this hypothesis is the observation that conditions independently associated with lower ILC abundance, such as HIV-1 infection (Kløverpris et al., 2016; Wang et al., 2020) and obesity (Brestoff et al., 2015; Yudanin et al., 2019), increase the risk for worse outcomes from SARS-CoV-2 infection (Biccard et al., 2021; Kompaniyets, 2021; Tesoriero et al., 2021).

In contrast to individuals with COVID-19, children with MIS-C had lower numbers

of T cells as well as ILCs (Table 5 and Fig. 4A,B), and longitudinal follow-up samples for pediatric COVID-19 and MIS-C patients showed persistence of low ILC numbers after COVID-19, but normalization of all depleted cell types after recovery from MIS-C (Fig. 4D,E and Supplementary Fig. S4). These differences imply that the reversible lymphopenia in MIS-C is due to different underlying processes than the more specific and persistent lower ILC abundance seen in individuals with COVID-19. This difference is made more interesting by the fact that none of the children with MIS-C had required hospitalization for COVID-19 and only one experienced any COVID-19 symptoms. The other children with MIS-C were therefore unaware that they had been infected. It is possible that children with pre-existing lower ILC numbers are at risk of developing COVID-19 if infected with SARS-CoV-2, while other factors such as prolonged exposure to SARS-CoV-2 antigens in the gastrointestinal tract (Yonker et al., 2021), or rare inborn errors of immunity (Sancho-Shimizu et al., 2021), promote inflammatory processes in MIS-C that drive nonspecific lymphoid cell depletion, which ultimately normalizes after recovery.

Although ILC depletion and recovery has been reported in rheumatoid arthritis (Rauber et al., 2017), inflammation-driven ILC-depletion is not necessarily reversible, as ILCs appear permanently depleted after HIV-1 infection, possibly by high levels of common γ-chain cytokines during acute infection (Wang et al., 2020). Better understanding of the processes that drive down ILC abundance in populations susceptible to COVID-19 could potentially allow for development of interventions that increase ILC abundance and restore homeostatic disease tolerance mechanisms.

In conclusion, considering the established homeostatic function of ILCs (Artis and

Spits, 2015; Branzk et al., 2018; Klose and Artis, 2016; Monticelli et al., 2015, 2011) and presumed non-immunologic, host adaptive responses necessary to survive pathogenic infection (López-Otín and Kroemer, 2021; McCarville and Ayres, 2018; Medzhitov et al., 2012; Schneider and Ayres, 2008), the findings reported here support the hypothesis that loss of disease tolerance mechanisms attributable to ILCs increase the risk of morbidity and mortality with SARS-CoV-2 infection. The findings of this observational study warrant establishment of prospective cohorts to determine whether abundance of ILCs or of other lymphoid cell subsets associated with disease tolerance (Arpaia et al., 2015; Artis and Spits, 2015; Branzk et al., 2018; Diefenbach et al., 2020; McCarville and Ayres, 2018; Monticelli et al., 2015, 2011), predict clinical outcome for infection with SARS-CoV-2 or other lethal pathogens. Understanding the mechanisms that allow an individual to tolerate high-level viral replication without experiencing symptoms, and how these mechanisms can fail and thereby allow for progression to severe disease, will provide the foundation for development of therapeutic interventions that maintain health and improve survival of pathogenic viral infection (Ayres, 2020b).

Materials and Methods

Data availability

The data that support the findings of this study are available within the manuscript and in its supplementary information files. Bulk RNA-seq datasets generated here can be found at: NCBI Gene Expression Omnibus (GEO): GSE168212. Bulk RNA-seq data generated by previously-published studies are available from NCBI GEO: GSE131031 and GSE126107. This study did not generate unique code. Any additional information required to reanalyze the data reported in this paper is available from the lead contact upon request.

Peripheral blood PBMCs

As part of a COVID-19 observational study, peripheral blood samples were collected from 91 adults with SARS-CoV-2 infection at the Massachusetts General Hospital and affiliated outpatient clinics. Request for access to coded patient samples was reviewed by the Massachusetts Consortium for Pathogen Readiness (https://masscpr.hms.harvard.edu/), and approved by the University of Massachusetts Medical School IRB (protocol #H00020836). Pediatric participants with COVID-19 or MIS-C were enrolled in the Massachusetts General Hospital Pediatric COVID-19 Biorepository (MGB IRB # 2020P000955); healthy pediatric controls were enrolled in the Pediatric Biorepository (MGB IRB # 2016P000949). Samples were collected after obtaining consent from the patient if 18 years or older, or from the parent/guardian, plus assent when appropriate. Demographic, laboratory, and clinical outcome data were included with the coded samples. Samples from 86 adult blood donors and 17 pediatric blood donors, either

collected prior to the SARS-CoV-2 outbreak, or from healthy individuals screened at a blood bank, were included as controls.

Human mononuclear cell isolation

Human peripheral blood was diluted in an equal volume of RPMI-1640 (Gibco), overlaid on Lymphoprep (STEMSELL, 07851), and centrifuged at 500 x g at room temperature for 30 minutes. Mononuclear cells were washed 3 times with MACS buffer (0.5% BSA and 2 mM EDTA in PBS) and frozen in FBS containing 10% DMSO.

Flow cytometry

Peripheral blood mononuclear cells (PBMCs) were first stained with Live and Dead violet viability kit (Invitrogen, L-34963). To detect surface molecules, cells were stained in MACS buffer with antibodies (Supplementary Table S8) for 30 min at 4°C in the dark. To detect IL-13 or AREG, cells were stimulated with PMA and ionomycin (eBioscience, 00-4970-03) for 3 hours with Brefeldin A and Monensin (eBioscience, 00-4980-03) present during the stimulation. To detect transcription factors or cytokines, cells were fixed and permeabilized using Foxp3 staining buffer kit (eBioscience, 00-5523-00), then intracellular molecules were stained in permeabilization buffer with antibodies. Cells were detected on a BD Celesta flow cytometer using previously established gating strategies (Wang et al., 2020). Cell subsets were identified using FlowJo™ software (Becton, Dickson and Company). Representative gating strategies are shown in Fig. S6.

692 **Bulk RNA-Seq Library preparation of PBMC ILCs**

693 The sequencing libraries were prepared using CEL-Seq2 (Hashimshony et al., 2016).
694 RNA from sorted cells was extracted using TRIzol reagent (ThermoFisher, 15596018).
695 10 ng RNA was used for first strand cDNA synthesis using barcoded primers (the specific
696 primers for each sample were listed in Supplementary Table S9). The second strand was
697 synthesized by NEBNext Second Strand Synthesis Module (NEB, E6111L). The pooled
698 dsDNA was purified with AMPure XP beads (Beckman Coulter, A63880), and subjected
699 to in vitro transcription (IVT) using HiScribe T7 High Yield RNA Synthesis Kit (NEB,
700 E2040S), then treated with ExoSAP-IT (Affymetrix, 78200). IVT RNA was fragmented
701 using RNA fragmentation reagents (Ambion), and underwent another reverse
702 transcription step using random hexamer RT primer-5'-GCC TTG GCA CCC GAG AAT
703 TCC ANN NNN N-3' to incorporate the second adapter. The final library was amplified
704 with indexed primers: RP1 and RPI1 (Supplementary Table S9), and the bead purified
705 library was quantified with 4200 TapeStation (Agilent Technologies), and paired-end
706 sequenced on Nextseq 500 V2 (Illumina), Read 1: 15 cycles; index 1: 6 cycles; Read 2:
707 60 cycles.
708
709 **RNA-seq analyses**
710 Pooled reads from PBMC ILCs were separated by CEL-Seq2 barcodes, and
711 demultiplexed reads from RNA-seq of ILCs from lung (Ardain et al., 2019), spleen and
712 intestine (Yudanin et al., 2019), were downloaded from GSE131031 and GSE126107.
713 Within the DolphinNext RNA-seq pipeline (Revision 4) (Yukselen et al., 2020), reads were
714 aligned to the hg19 genome using STAR (version 2.1.6) (Dobin et al., 2013) and counts

of reads aligned to RefSeq genes were quantified using RSEM (version 1.3.1) (Li and Dewey, 2011). Normalized transcript abundance in the form of TPMs were used to filter out low abundance transcripts with an average of <3 TPMs across libraries. RSEM-generated expected counts were normalized and differential analysis was performed using DEseq2 (Love et al., 2014) in R, with significant genes defined as a greater than 1.5-fold difference and an adjusted p-value <0.01. GO Enrichment Analysis was performed in R using the enrichGO function in the clusterProfiler R package (Yu et al., 2012). Data were transformed using vsd within DEseq2 both for the heatmap visualization with ComplexHeatmap (Gu et al., 2016) and for principal component analysis (PCA) with prcomp on the top 250 most variable genes. Normalized counts were generated for plotting using the counts command in Deseq2.

Statistical analysis and data visualization

Data were prepared for analysis with tidyverse packages (Wickham et al., 2019) and visualized using the ggplot2 (Wickham, 2016), ggpubr (Kassambara, 2020), and ComplexHeatmap (Gu et al., 2016) packages, within the R computer software environment (version 4.0.2) (R Core Team, 2020). Group differences were determined with pairwise, two-sided, Wilcoxon rank-sum tests, or Fisher's exact test, as indicated, with Bonferroni correction for multiple comparisons. Multiple linear regression analyses were performed with dependent and independent variables as indicated in the text, using the lm function in R. Pairwise group comparisons on estimated marginal means generated from multiple linear regression were performed using the emmeans package (Lenth, 2020) in R, with multiple comparison correction using the Tukey adjustment. Multiple logistic regressions were performed using the glm function in R. Longitudinal

follow-up analyses on pediatric COVID-19 and MIS-C was performed with linear mixed-effect models using lme4 (Bates et al., 2015) in R with the equation: log2 (lymphoid cell abundance) ~ Age + Sex + Group + Group:Follow_up + (1|Patient_ID). This model tested the effect of followup on ILC abundance in the pediatric COVID-19 and MIS-C groups while accounting for age, sex, and group. Statistical significance was determined with lmerTest (Kuznetsova et al., 2017) in R, using the Satterthwarte's degrees of freedom method. $p<0.05$ was considered significant. United States SARS-CoV-2 infection and mortality data were downloaded from (CDC Case Surveillance Task Force, 2020) and cases with age group and outcome available were plotted by age group as indicated. Mortality rate was calculated by dividing the number of fatal cases by the total number of cases with known outcome in each age group as indicated.

REFERENCES

Alghamdi IG, Hussain II, Almalki SS, Alghamdi MS, Alghamdi MM, El-Sheemy MA. 2014. The pattern of Middle East respiratory syndrome coronavirus in Saudi Arabia: a descriptive epidemiological analysis of data from the Saudi Ministry of Health. *Int J Gen Med* **7**:417.

Alkhouli M, Nanjundappa A, Annie F, Bates MC, Bhatt DL. 2020. Sex Differences in Case Fatality Rate of COVID-19: Insights From a Multinational Registry. *Mayo Clin Proc* **95**:1613–1620.

Anegon I, Cuturi MC, Trinchieri G, Perussia B. 1988. Interaction of Fc receptor (CD16) ligands induces transcription of interleukin 2 receptor (CD25) and lymphokine genes and expression of their products in human natural killer cells. *J Exp Med* **167**:452–472.

Ardain A, Domingo-Gonzalez R, Das S, Kazer SW, Howard NC, Singh A, Ahmed M, Nhamoyebonde S, Rangel-Moreno J, Ogongo P, Lu L, Ramsuran D, de la Luz Garcia-Hernandez M, K. Ulland T, Darby M, Park E, Karim F, Melocchi L, Madansein R, Dullabh KJ, Dunlap M, Marin-Agudelo N, Ebihara T, Ndung'u T, Kaushal D, Pym AS, Kolls JK, Steyn A, Zúñiga J, Horsnell W, Yokoyama WM, Shalek AK, Kløverpris HN, Colonna M, Leslie A, Khader SA. 2019. Group 3 innate lymphoid cells mediate early protective immunity against tuberculosis. *Nature* **570**:528–532.

Arpaia N, Green JA, Moltedo B, Arvey A, Hemmers S, Yuan S, Treuting PM, Rudensky AY. 2015. A Distinct Function of Regulatory T Cells in Tissue Protection. *Cell* **162**:1078–1089.

783 Artis D, Spits H. 2015. The biology of innate lymphoid cells. *Nature* **517**:293–301.

784 Ayres JS. 2020a. The Biology of Physiological Health. *Cell* **181**:250–269.

785 Ayres JS. 2020b. Surviving COVID-19: A disease tolerance perspective. *Sci Adv*
786 **6**:eabc1518.

787 Bates D, Mächler M, Bolker B, Walker S. 2015. Fitting Linear Mixed-Effects Models
788 Usinglme4. *Journal of Statistical Software*. doi:10.18637/jss.v067.i01

789 Biccard BM, Gopalan PD, Miller M, Michell WL, Thomson D, Ademuyiwa A, Aniteye E,
790 Calligaro G, Chaibou MS, Dhufera HT, Elfagieh M, Elfiky M, Elhadi M, Fawzy M,
791 Fredericks D, Gebre M, Bayih AG, Hardy A, Joubert I, Kifle F, Kluyts H-L, Macleod
792 K, Mekonnen Z, Mer M, Morais A, Msosa V, Mulwafu W, Ndonga A, Ngumi Z,
793 Omigbodun A, Owoo C, Paruk F, Piercy JL, Scribante J, Seman Y, Taylor E, van
794 Straaten D, Elfiky M, Fawzy M, Awad A, Hussein H, Shaban M, Elbadawy M,
795 Elmehrath AO, Cordie A, Elganainy M, El-Shazly M, Essam M, Abdelwahab OA,
796 Ali A, Hussein AM, Kamel EZ, Monib FA, Ahmed I, Saad MM, Al-Quossi MA,
797 Rafaat N, Galal I, Labib B, Omran DO, Fawzy M, Elfiky M, Azzam Ahmed, Azab
798 M, Tawheed A, Gamal M, El Kassas M, Azzam Aml, Ahmed N, NasrEldin Y,
799 Abdewahab O, Elganainy M, Elmandouh O, Dhufera HT, MeGebre M, Bayih AG,
800 Kifle F, Mekonnen Z, Seman Y, Addisie A, Eshete A, Kifle F, Desita K, Araya H,
801 Agidew Y, Andabo AD, Tesfaye E, Yesuf EA, Hailemariam G, Mohammed MS,
802 Gebremedhin Y, Taye Y, Mebrate TA, Gemechu TB, Bedane TT, Abera ET,
803 Teshome A, Ernest Aniteye EA, Christian Owoo CO, Doku A, Owoo C, Afriyie-
804 Mensah JS, Lawson A, Owoo C, DYaw Sottie DA, Addae E, Ernest Ofosu-Appiah
805 EO-A, William Obeng WO, Ndonga A, Ngumi Z, Ndonga A, Mugera A, Bitta C,

Elfagieh M, Elhadi M, Huwaysh MA, Yahya MMA, Mohammed AAK, Majeed AAM, Mohammed AEM, Majeed E, Abusalama AA, Altayr E, Abubaker T, Alkaseek AM, Abdulhafith B, Alziyituni Z, Gamra MF, Anaiba MM, Khel S, Abdelkabir M, Abdeewi S, Adam S, Alhadi A, Alsoufi A, Hassan M, Msherghi A, Bouhuwaish AEM, Msosa V, Mulwafu W, Masoo F, Chikumbanje SS, Mabedi D, Morais A, Carlos A, Morais A, Lorenzoni C, Mambo J, Isabel Chissaque I, Mouzinho Saide M, Chaibou MS, Mamane M, Amadou F, Adesoji Ademuyiwa AA, Akinyinka Omigbodun AO, Adeyeye A, Akinmade A, Momohsani Y, Bamigboye J, Orshio D, Isamade ES, Embu H, Nuhu S, Ojiakor S, Nuhu A, Fowotade A, Sanusi A, Osinaike B, Idowu O, Amali AO, Ibrahim S, Adamu AA, Kida I, Otokwala J, Essam M, Alagbe-Briggs O, Ojum S, Fathima Paruk FP, Juan Scribante JS, Mdladla A, Mabotja T, Naidoo R, Matos-Puig R, Ramkillawan A, Smith M, Arnold-Day C, Thomson D, Calligaro G, Joubert I, Jagga J, Piercy J, Michell L, Devenish L, Miller M, Fernandes N, Gopalan D, Pershad S, Grabowski N, Rammego M, Zwane S, Dhlamini ME, Neuhoff M, Fodo T, Usenbo A, Mrara B, Kabambi F, Cloete E, De Caires L, Dickerson R, Louw C, Theron A, Herselman R, Badenhorst J, Moletsane G, Loots H, Paruk F, Chausse J, Neuhoff M, Sebastian M, Grabowski N, Rheeder P, van Hougenhouck-Tulleken W, Snyman C, Adeleke D, Esterhuizen J, de Man L, Mosola M, van der Linde P, Swart R, Maasdorp S, Martins T, Govender V. 2021. Patient care and clinical outcomes for patients with COVID-19 infection admitted to African high-care or intensive care units (ACCCOS): a multicentre, prospective, observational cohort study. *Lancet* **397**:1885–1894.

828 Branzk N, Gronke K, Diefenbach A. 2018. Innate lymphoid cells, mediators of tissue
829 homeostasis, adaptation and disease tolerance. *Immunol Rev* **286**:86–101.
830 Brestoff JR, Kim BS, Saenz SA, Stine RR, Monticelli LA, Sonnenberg GF, Thome JJ,
831 Farber DL, Lutfy K, Seale P, Artis D. 2015. Group 2 innate lymphoid cells promote
832 beiging of white adipose tissue and limit obesity. *Nature* **519**:242–246.
833 Bunders MJ, Altfeld M. 2020. Implications of Sex Differences in Immunity for SARS-CoV-
834 2 Pathogenesis and Design of Therapeutic Interventions. *Immunity* **53**:487–495.
835 Califano D, Furuya Y, Roberts S, Avram D, McKenzie ANJ, Metzger DW. 2018. IFN-γ
836 increases susceptibility to influenza A infection through suppression of group II
837 innate lymphoid cells. *Mucosal Immunol* **11**:209–219.
838 CDC Case Surveillance Task Force. 2020. COVID-19 Case Surveillance Public Use
839 Data.
840 Cevik M, Tate M, Lloyd O, Maraolo AE, Schafers J, Ho A. 2021. SARS-CoV-2, SARS-
841 CoV, and MERS-CoV viral load dynamics, duration of viral shedding, and
842 infectiousness: a systematic review and meta-analysis. *The Lancet Microbe*
843 **2**:e13–e22.
844 Channappanavar R, Fett C, Mack M, Ten Eyck PP, Meyerholz DK, Perlman S. 2017. Sex-
845 Based Differences in Susceptibility to Severe Acute Respiratory Syndrome
846 Coronavirus Infection. *J Immunol* **198**:4046–4053.
847 Charles Bailey L, Razzaghi H, Burrows EK, Timothy Bunnell H, Camacho PEF, Christakis
848 DA, Eckrich D, Kitzmiller M, Lin SM, Magnusen BC, Newland J, Pajor NM, Ranade
849 D, Rao S, Sofela O, Zahner J, Bruno C, Forrest CB. 2020. Assessment of 135 794

Pediatric Patients Tested for Severe Acute Respiratory Syndrome Coronavirus 2 Across the United States. *JAMA Pediatr*. doi:10.1001/jamapediatrics.2020.5052

Chen G, Wu D, Guo W, Cao Y, Huang D, Wang H, Wang T, Zhang Xiaoyun, Chen H, Yu H, Zhang Xiaoping, Zhang M, Wu S, Song J, Chen T, Han M, Li S, Luo X, Zhao J, Ning Q. 2020. Clinical and immunological features of severe and moderate coronavirus disease 2019. *J Clin Invest* **130**:2620–2629.

Chen J, Subbarao K. 2007. The Immunobiology of SARS. *Annu Rev Immunol* **25**:443–472.

Cherrier DE, Serafini N, Di Santo JP. 2018. Innate Lymphoid Cell Development: A T Cell Perspective. *Immunity* **48**:1091–1103.

Cheung EW, Zachariah P, Gorelik M, Boneparth A, Kernie SG, Orange JS, Milner JD. 2020. Multisystem Inflammatory Syndrome Related to COVID-19 in Previously Healthy Children and Adolescents in New York City. *JAMA* **324**:294–296.

Cumnock K, Gupta AS, Lissner M, Chevee V, Davis NM, Schneider DS. 2018. Host Energy Source Is Important for Disease Tolerance to Malaria. *Curr Biol* **28**:1635-1642.e3.

Darboe A, Nielsen CM, Wolf A-S, Wildfire J, Danso E, Sonko B, Bottomley C, Moore SE, Riley EM, Goodier MR. 2020. Age-Related Dynamics of Circulating Innate Lymphoid Cells in an African Population. *Front Immunol* **11**:594107.

Diefenbach A, Gnafakis S, Shomrat O. 2020. Innate Lymphoid Cell-Epithelial Cell Modules Sustain Intestinal Homeostasis. *Immunity* **52**:452–463.

871 Dobin A, Davis CA, Schlesinger F, Drenkow J, Zaleski C, Jha S, Batut P, Chaisson M,
872 Gingeras TR. 2013. STAR: ultrafast universal RNA-seq aligner. *Bioinformatics*
873 **29**:15–21.
874 Donnelly CA, Ghani AC, Leung GM, Hedley AJ, Fraser C, Riley S, Abu-Raddad LJ, Ho
875 L-M, Thach T-Q, Chau P, Chan K-P, Lam T-H, Tse L-Y, Tsang T, Liu S-H, Kong
876 JHB, Lau EMC, Ferguson NM, Anderson RM. 2003. Epidemiological determinants
877 of spread of causal agent of severe acute respiratory syndrome in Hong Kong.
878 *Lancet* **361**:1761–1766.
879 D'Souza SS, Shen X, Fung ITH, Ye L, Kuentzel M, Chittur SV, Furuya Y, Siebel CW,
880 Maillard IP, Metzger DW, Yang Q. 2019. Compartmentalized effects of aging on
881 group 2 innate lymphoid cell development and function. *Aging Cell*.
882 doi:10.1111/acel.13019
883 Feldstein LR, Rose EB, Horwitz SM, Collins JP, Newhams MM, Son MBF, Newburger
884 JW, Kleinman LC, Heidemann SM, Martin AA, Singh AR, Li S, Tarquinio KM, Jaggi
885 P, Oster ME, Zackai SP, Gillen J, Ratner AJ, Walsh RF, Fitzgerald JC, Keenaghan
886 MA, Alharash H, Doymaz S, Clouser KN, Giuliano JS Jr, Gupta A, Parker RM,
887 Maddux AB, Havalad V, Ramsingh S, Bukulmez H, Bradford TT, Smith LS,
888 Tenforde MW, Carroll CL, Riggs BJ, Gertz SJ, Daube A, Lansell A, Coronado
889 Munoz A, Hobbs CV, Marohn KL, Halasa NB, Patel MM, Randolph AG,
890 Overcoming COVID-19 Investigators, CDC COVID-19 Response Team. 2020.
891 Multisystem Inflammatory Syndrome in U.S. Children and Adolescents. *N Engl J*
892 *Med* **383**:334–346.

893 Feldstein LR, Tenforde MW, Friedman KG, Newhams M, Rose EB, Dapul H, Soma VL,
894 Maddux AB, Mourani PM, Bowens C, Maamari M, Hall MW, Riggs BJ, Giuliano JS
895 Jr, Singh AR, Li S, Kong M, Schuster JE, McLaughlin GE, Schwartz SP, Walker
896 TC, Loftis LL, Hobbs CV, Halasa NB, Doymaz S, Babbitt CJ, Hume JR, Gertz SJ,
897 Irby K, Clouser KN, Cvijanovich NZ, Bradford TT, Smith LS, Heidemann SM,
898 Zackai SP, Wellnitz K, Nofziger RA, Horwitz SM, Carroll RW, Rowan CM,
899 Tarquinio KM, Mack EH, Fitzgerald JC, Coates BM, Jackson AM, Young CC, Son
900 MBF, Patel MM, Newburger JW, Randolph AG, Overcoming COVID-19
901 Investigators. 2021. Characteristics and Outcomes of US Children and
902 Adolescents With Multisystem Inflammatory Syndrome in Children (MIS-C)
903 Compared With Severe Acute COVID-19. *JAMA*. doi:10.1001/jama.2021.2091
904 Flanagan KL, Fink AL, Plebanski M, Klein SL. 2017. Sex and Gender Differences in the
905 Outcomes of Vaccination over the Life Course. *Annu Rev Cell Dev Biol* **33**:577–
906 599.
907 Gallo Marin B, Aghagoli G, Lavine K, Yang L, Siff EJ, Chiang SS, Salazar-Mather TP,
908 Dumenco L, Savaria MC, Aung SN, Flanigan T, Michelow IC. 2020. Predictors of
909 COVID-19 severity: A literature review. *Rev Med Virol* e2146.
910 García M, Kokkinou E, Carrasco García A, Parrot T, Palma Medina LM, Maleki KT, Christ
911 W, Varnaitė R, Filipovic I, Ljunggren H-G, Others. 2020. Innate lymphoid cell
912 composition associates with COVID-19 disease severity. *Clinical & translational*
913 *immunology* **9**:e1224.

914 Giefing-Kröll C, Berger P, Lepperdinger G, Grubeck-Loebenstein B. 2015. How sex and
915 age affect immune responses, susceptibility to infections, and response to
916 vaccination. *Aging Cell* **14**:309–321.
917 Gu Z, Eils R, Schlesner M. 2016. Complex heatmaps reveal patterns and correlations in
918 multidimensional genomic data. *Bioinformatics* **32**:2847–2849.
919 Gupta RK, Harrison EM, Ho A, Docherty AB, Knight SR, van Smeden M, Abubakar I,
920 Lipman M, Quartagno M, Pius R, Buchan I, Carson G, Drake TM, Dunning J,
921 Fairfield CJ, Gamble C, Green CA, Halpin S, Hardwick HE, Holden KA, Horby PW,
922 Jackson C, Mclean KA, Merson L, Nguyen-Van-Tam JS, Norman L, Olliaro PL,
923 Pritchard MG, Russell CD, Scott-Brown J, Shaw CA, Sheikh A, Solomon T, Sudlow
924 C, Swann OV, Turtle L, Openshaw PJM, Baillie JK, Semple MG, Noursadeghi M,
925 ISARIC4C Investigators. 2021. Development and validation of the ISARIC 4C
926 Deterioration model for adults hospitalised with COVID-19: a prospective cohort
927 study. *Lancet Respir Med*. doi:10.1016/S2213-2600 (20)30559-2
928 Hashimshony T, Senderovich N, Avital G, Klochendler A, de Leeuw Y, Anavy L, Gennert
929 D, Li S, Livak KJ, Rozenblatt-Rosen O, Dor Y, Regev A, Yanai I. 2016. CEL-Seq2:
930 sensitive highly-multiplexed single-cell RNA-Seq. *Genome Biol* **17**:77.
931 He J, Guo Y, Mao R, Zhang J. 2021. Proportion of asymptomatic coronavirus disease
932 2019: A systematic review and meta-analysis. *J Med Virol* **93**:820–830.
933 Heald-Sargent T, Muller WJ, Zheng X, Rippe J, Patel AB, Kociolek LK. 2020. Age-Related
934 Differences in Nasopharyngeal Severe Acute Respiratory Syndrome Coronavirus
935 2 (SARS-CoV-2) Levels in Patients With Mild to Moderate Coronavirus Disease
936 2019 (COVID-19). *JAMA Pediatr* **174**:902–903.

937 Huang C, Wang Y, Li X, Ren L, Zhao J, Hu Y, Zhang L, Fan G, Xu J, Gu X, Cheng Z, Yu
938 T, Xia J, Wei Y, Wu W, Xie X, Yin W, Li H, Liu M, Xiao Y, Gao H, Guo L, Xie J,
939 Wang G, Jiang R, Gao Z, Jin Q, Wang J, Cao B. 2020. Clinical features of patients
940 infected with 2019 novel coronavirus in Wuhan, China. *Lancet* **395**:497–506.
941 Huang I, Pranata R. 2020. Lymphopenia in severe coronavirus disease-2019 (COVID-
942 19): systematic review and meta-analysis. *J Intensive Care Med* **8**:36.
943 Jamieson AM, Pasman L, Yu S, Gamradt P, Homer RJ, Decker T, Medzhitov R. 2013.
944 Role of tissue protection in lethal respiratory viral-bacterial coinfection. *Science*
945 **340**:1230–1234.
946 Jhaveri KA, Trammell RA, Toth LA. 2007. Effect of environmental temperature on sleep,
947 locomotor activity, core body temperature and immune responses of C57BL/6J
948 mice. *Brain Behav Immun* **21**:975–987.
949 Jones TC, Biele G, Mühlemann B, Veith T, Schneider J, Beheim-Schwarzbach J, Bleicker
950 T, Tesch J, Schmidt ML, Sander LE, Kurth F, Menzel P, Schwarzer R, Zuchowski
951 M, Hofmann J, Krumbholz A, Stein A, Edelmann A, Corman VM, Drosten C. 2021.
952 Estimating infectiousness throughout SARS-CoV-2 infection course. *Science*
953 **373**:eabi5273.
954 Karlberg J. 2004. Do Men Have a Higher Case Fatality Rate of Severe Acute Respiratory
955 Syndrome than Women Do? *American Journal of Epidemiology*.
956 doi:10.1093/aje/kwh056
957 Kassambara A. 2020. ggpubr: “ggplot2” Based Publication Ready Plots.
958 Klein SL, Flanagan KL. 2016. Sex differences in immune responses. *Nat Rev Immunol*
959 **16**:626–638.

960 Klose CSN, Artis D. 2016. Innate lymphoid cells as regulators of immunity, inflammation
961 and tissue homeostasis. *Nat Immunol* **17**:765–774.
962 Kløverpris HN, Kazer SW, Mjösberg J, Mabuka JM, Wellmann A, Ndhlovu Z, Yadon MC,
963 Nhamoyebonde S, Muenchhoff M, Simoni Y, Andersson F, Kuhn W, Garrett N,
964 Burgers WA, Kamya P, Pretorius K, Dong K, Moodley A, Newell EW, Kasprowicz
965 V, Abdool Karim SS, Goulder P, Shalek AK, Walker BD, Ndung'u T, Leslie A. 2016.
966 Innate Lymphoid Cells Are Depleted Irreversibly during Acute HIV-1 Infection in
967 the Absence of Viral Suppression. *Immunity* **44**:391–405.
968 Kompaniyets L. 2021. Body Mass Index and Risk for COVID-19–Related Hospitalization,
969 Intensive Care Unit Admission, Invasive Mechanical Ventilation, and Death —
970 United States, March–December 2020. *MMWR Morb Mortal Wkly Rep* **70**.
971 doi:10.15585/mmwr.mm7010e4
972 Kuri-Cervantes L, Pampena MB, Meng W, Rosenfeld AM, Ittner CAG, Weisman AR,
973 Agyekum RS, Mathew D, Baxter AE, Vella LA, Kuthuru O, Apostolidis SA, Bershaw
974 L, Dougherty J, Greenplate AR, Pattekar A, Kim J, Han N, Gouma S, Weirick ME,
975 Arevalo CP, Bolton MJ, Goodwin EC, Anderson EM, Hensley SE, Jones TK,
976 Mangalmurti NS, Luning Prak ET, Wherry EJ, Meyer NJ, Betts MR. 2020.
977 Comprehensive mapping of immune perturbations associated with severe COVID-
978 19. *Sci Immunol* **5**:eabd7114.
979 Kuznetsova A, Brockhoff PB, Christensen RHB, Others. 2017. lmerTest package: tests
980 in linear mixed effects models. *J Stat Softw* **82**:1–26.

981 Laxminarayan R, Wahl B, Dudala SR, Gopal K, Mohan B C, Neelima S, Jawahar Reddy
982 KS, Radhakrishnan J, Lewnard JA. 2020. Epidemiology and transmission
983 dynamics of COVID-19 in two Indian states. *Science* **370**:691–697.
984 Lee S, Kim T, Lee E, Lee C, Kim H, Rhee H, Park SY, Son H-J, Yu S, Park JW, Choo EJ,
985 Park S, Loeb M, Kim TH. 2020. Clinical Course and Molecular Viral Shedding
986 Among Asymptomatic and Symptomatic Patients With SARS-CoV-2 Infection in a
987 Community Treatment Center in the Republic of Korea. *JAMA Internal Medicine*
988 **180**:1447.
989 Leist SR, Dinnon KH 3rd, Schäfer A, Tse LV, Okuda K, Hou YJ, West A, Edwards CE,
990 Sanders W, Fritch EJ, Gully KL, Scobey T, Brown AJ, Sheahan TP, Moorman NJ,
991 Boucher RC, Gralinski LE, Montgomery SA, Baric RS. 2020. A Mouse-Adapted
992 SARS-CoV-2 Induces Acute Lung Injury and Mortality in Standard Laboratory
993 Mice. *Cell* **183**:1070-1085.e12.
994 Lennon NJ, Bhattacharyya RP, Mina MJ, Rehm HL, Hung DT, Smole S, Woolley A,
995 Lander ES, Gabriel SB. 2021. Cross-sectional assessment of SARS-CoV-2 viral
996 load by symptom status in Massachusetts congregate living facilities. *J Infect Dis*.
997 doi:10.1093/infdis/jiab367
998 Lennon NJ, Bhattacharyya RP, Mina MJ, Rehm HL, Hung DT, Smole S, Woolley A,
999 Lander ES, Gabriel SB. 2020. Comparison of viral levels in individuals with or
1000 without symptoms at time of COVID-19 testing among 32,480 residents and staff
1001 of nursing homes and assisted living facilities in Massachusetts. *bioRxiv*.
1002 doi:10.1101/2020.07.20.20157792
1003 Lenth R. 2020. emmeans: Estimated Marginal Means, aka Least-Squares Means.

1004 Li B, Dewey CN. 2011. RSEM: accurate transcript quantification from RNA-Seq data with
1005 or without a reference genome. *BMC Bioinformatics* **12**:323.
1006 Li B, Zhang S, Zhang R, Chen X, Wang Y, Zhu C. 2020. Epidemiological and Clinical
1007 Characteristics of COVID-19 in Children: A Systematic Review and Meta-Analysis.
1008 *Front Pediatr* **8**:591132.
1009 Licciardi F, Pruccoli G, Denina M, Parodi E, Taglietto M, Rosati S, Montin D. 2020. SARS-
1010 CoV-2-Induced Kawasaki-Like Hyperinflammatory Syndrome: A Novel COVID
1011 Phenotype in Children. *Pediatrics*. doi:10.1542/peds.2020-1711
1012 López-Otín C, Kroemer G. 2021. Hallmarks of Health. *Cell* **184**:33–63.
1013 LoTempio JE, Billings EA, Draper K, Ralph C, Moshgriz M, Duong N, Bard JD, Gai X,
1014 Wessel D, DeBiasi RL, Campos JM, Vilain E, Delaney M, Michael DG. 2021. Novel
1015 SARS-CoV-2 spike variant identified through viral genome sequencing of the
1016 pediatric Washington D.C. COVID-19 outbreak. *medRxiv* 2021.02.08.21251344.
1017 Love M, Anders S, Huber W. 2014. Differential analysis of count data--the DESeq2
1018 package. *Genome Biol* **15**:550.
1019 Lu X, Zhang L, Du H, Zhang J, Li YY, Qu J, Zhang W, Wang Y, Bao S, Li Y, Wu C, Liu H,
1020 Liu D, Shao J, Peng X, Yang Y, Liu Z, Xiang Y, Zhang F, Silva RM, Pinkerton KE,
1021 Shen K, Xiao H, Xu S, Wong GWK, Chinese Pediatric Novel Coronavirus Study
1022 Team. 2020. SARS-CoV-2 Infection in Children. *N Engl J Med* **382**:1663–1665.
1023 Lucas C, Wong P, Klein J, Castro TBR, Silva J, Sundaram M, Ellingson MK, Mao T, Oh
1024 JE, Israelow B, Takahashi T, Tokuyama M, Lu P, Venkataraman A, Park A,
1025 Mohanty S, Wang H, Wyllie AL, Vogels CBF, Earnest R, Lapidus S, Ott IM, Moore
1026 AJ, Muenker MC, Fournier JB, Campbell M, Odio CD, Casanovas-Massana A,

Yale IMPACT Team, Herbst R, Shaw AC, Medzhitov R, Schulz WL, Grubaugh ND, Dela Cruz C, Farhadian S, Ko AI, Omer SB, Iwasaki A. 2020. Longitudinal analyses reveal immunological misfiring in severe COVID-19. *Nature* **584**:463–469.

Luo X, Zhou W, Yan X, Guo T, Wang B, Xia H, Ye L, Xiong J, Jiang Z, Liu Y, Zhang B, Yang W. 2020. Prognostic Value of C-Reactive Protein in Patients With Coronavirus 2019. *Clin Infect Dis* **71**:2174–2179.

Márquez EJ, Chung C-H, Marches R, Rossi RJ, Nehar-Belaid D, Eroglu A, Mellert DJ, Kuchel GA, Banchereau J, Ucar D. 2020. Sexual-dimorphism in human immune system aging. *Nat Commun* **11**:751.

Mathew D, Giles JR, Baxter AE, Oldridge DA, Greenplate AR, Wu JE, Alanio C, Kuri-Cervantes L, Pampena MB, D'Andrea K, Manne S, Chen Z, Huang YJ, Reilly JP, Weisman AR, Ittner CAG, Kuthuru O, Dougherty J, Nzingha K, Han N, Kim J, Pattekar A, Goodwin EC, Anderson EM, Weirick ME, Gouma S, Arevalo CP, Bolton MJ, Chen F, Lacey SF, Ramage H, Cherry S, Hensley SE, Apostolidis SA, Huang AC, Vella LA, UPenn COVID Processing Unit, Betts MR, Meyer NJ, Wherry EJ. 2020. Deep immune profiling of COVID-19 patients reveals distinct immunotypes with therapeutic implications. *Science* **369**. doi:10.1126/science.abc8511

Mauvais-Jarvis F. 2020. Aging, Male Sex, Obesity, and Metabolic Inflammation Create the Perfect Storm for COVID-19. *Diabetes* **69**:1857–1863.

McCarville JL, Ayres JS. 2018. Disease tolerance: concept and mechanisms. *Curr Opin Immunol* **50**:88–93.

1050 Medzhitov R, Schneider DS, Soares MP. 2012. Disease tolerance as a defense strategy.
1051 *Science* **335**:936–941.
1052 Monticelli LA, Osborne LC, Noti M, Tran SV, Zaiss DMW, Artis D. 2015. IL-33 promotes
1053 an innate immune pathway of intestinal tissue protection dependent on
1054 amphiregulin–EGFR interactions. *Proc Natl Acad Sci U S A* **112**:10762–10767.
1055 Monticelli LA, Sonnenberg GF, Abt MC, Alenghat T, Ziegler CGK, Doering TA,
1056 Angelosanto JM, Laidlaw BJ, Yang CY, Sathaliyawala T, Kubota M, Turner D,
1057 Diamond JM, Goldrath AW, Farber DL, Collman RG, Wherry EJ, Artis D. 2011.
1058 Innate lymphoid cells promote lung-tissue homeostasis after infection with
1059 influenza virus. *Nat Immunol* **12**:1045–1054.
1060 Mudd PA, Crawford JC, Turner JS, Souquette A, Reynolds D, Bender D, Bosanquet JP,
1061 Anand NJ, Striker DA, Martin RS, Boon ACM, House SL, Remy KE, Hotchkiss RS,
1062 Presti RM, O'Halloran JA, Powderly WG, Thomas PG, Ellebedy AH. 2020. Distinct
1063 inflammatory profiles distinguish COVID-19 from influenza with limited
1064 contributions from cytokine storm. *Sci Adv* **6**. doi:10.1126/sciadv.abe3024
1065 O'Driscoll M, Ribeiro Dos Santos G, Wang L, Cummings DAT, Azman AS, Paireau J,
1066 Fontanet A, Cauchemez S, Salje H. 2020. Age-specific mortality and immunity
1067 patterns of SARS-CoV-2. *Nature*. doi:10.1038/s41586-020-2918-0
1068 Patin E, Hasan M, Bergstedt J, Rouilly V, Libri V, Urrutia A, Alanio C, Scepanovic P,
1069 Hammer C, Jönsson F, Beitz B, Quach H, Lim YW, Hunkapiller J, Zepeda M,
1070 Green C, Piasecka B, Leloup C, Rogge L, Huetz F, Peguillet I, Lantz O, Fontes M,
1071 Di Santo JP, Thomas S, Fellay J, Duffy D, Quintana-Murci L, Albert ML, Milieu

1072 Intérieur Consortium. 2018. Natural variation in the parameters of innate immune
1073 cells is preferentially driven by genetic factors. *Nat Immunol* **19**:302–314.
1074 Peckham H, de Gruijter NM, Raine C, Radziszewska A, Ciurtin C, Wedderburn LR,
1075 Rosser EC, Webb K, Deakin CT. 2020. Male sex identified by global COVID-19
1076 meta-analysis as a risk factor for death and ITU admission. *Nature*
1077 *Communications* **11**:6317.
1078 Piasecka B, Duffy D, Urrutia A, Quach H, Patin E, Posseme C, Bergstedt J, Charbit B,
1079 Rouilly V, MacPherson CR, Hasan M, Albaud B, Gentien D, Fellay J, Albert ML,
1080 Quintana-Murci L, Milieu Intérieur Consortium. 2018. Distinctive roles of age, sex,
1081 and genetics in shaping transcriptional variation of human immune responses to
1082 microbial challenges. *Proc Natl Acad Sci U S A* **115**:E488–E497.
1083 Poline J, Gaschignard J, Leblanc C, Madhi F, Foucaud E, Nattes E, Faye A, Bonacorsi
1084 S, Mariani P, Varon E, Smati-Lafarge M, Caseris M, Basmaci R, Lachaume N,
1085 Ouldali N. 2020. Systematic SARS-CoV-2 screening at hospital admission in
1086 children:a French prospective multicenter study. *Clin Infect Dis*.
1087 doi:10.1093/cid/ciaa1044
1088 R Core Team. 2020. R: A Language and Environment for Statistical Computing.
1089 Ra SH, Lim JS, Kim G-U, Kim MJ, Jung J, Kim S-H. 2021. Upper respiratory viral load in
1090 asymptomatic individuals and mildly symptomatic patients with SARS-CoV-2
1091 infection. *Thorax* **76**:61–63.
1092 Råberg L, Sim D, Read AF. 2007. Disentangling genetic variation for resistance and
1093 tolerance to infectious diseases in animals. *Science* **318**:812–814.

1094 Rak GD, Osborne LC, Siracusa MC, Kim BS, Wang K, Bayat A, Artis D, Volk SW. 2016.
1095 IL-33-Dependent Group 2 Innate Lymphoid Cells Promote Cutaneous Wound
1096 Healing. *J Invest Dermatol* **136**:487–496.
1097 Rauber S, Luber M, Weber S, Maul L, Soare A, Wohlfahrt T, Lin N-Y, Dietel K, Bozec A,
1098 Herrmann M, Kaplan MH, Weigmann B, Zaiss MM, Fearon U, Veale DJ, Cañete
1099 JD, Distler O, Rivellese F, Pitzalis C, Neurath MF, McKenzie ANJ, Wirtz S, Schett
1100 G, Distler JHW, Ramming A. 2017. Resolution of inflammation by interleukin-9-
1101 producing type 2 innate lymphoid cells. *Nat Med* **23**:938–944.
1102 Richardson S, Hirsch JS, Narasimhan M, Crawford JM, McGinn T, Davidson KW, the
1103 Northwell COVID-19 Research Consortium, Barnaby DP, Becker LB, Chelico JD,
1104 Cohen SL, Cookingham J, Coppa K, Diefenbach MA, Dominello AJ, Duer-Hefele
1105 J, Falzon L, Gitlin J, Hajizadeh N, Harvin TG, Hirschwerk DA, Kim EJ, Kozel ZM,
1106 Marrast LM, Mogavero JN, Osorio GA, Qiu M, Zanos TP. 2020. Presenting
1107 Characteristics, Comorbidities, and Outcomes Among 5700 Patients Hospitalized
1108 With COVID-19 in the New York City Area. *JAMA* **323**:2052–2059.
1109 Riphagen S, Gomez X, Gonzalez-Martinez C, Wilkinson N, Theocharis P. 2020.
1110 Hyperinflammatory shock in children during COVID-19 pandemic. *Lancet*.
1111 Sanchez KK, Chen GY, Schieber AMP, Redford SE, Shokhirev MN, Leblanc M, Lee YM,
1112 Ayres JS. 2018. Cooperative Metabolic Adaptations in the Host Can Favor
1113 Asymptomatic Infection and Select for Attenuated Virulence in an Enteric
1114 Pathogen. *Cell* **175**:146-158.e15.
1115 Sancho-Shimizu V, Brodin P, Cobat A, Biggs CM, Toubiana J, Lucas CL, Henrickson SE,
1116 Belot A, MIS-C@CHGE, Tangye SG, Milner JD, Levin M, Abel L, Bogunovic D,

Casanova J-L, Zhang S-Y. 2021. SARS-CoV-2–related MIS-C: A key to the viral and genetic causes of Kawasaki disease? *J Exp Med* **218**. doi:10.1084/jem.20210446

Schneider DS, Ayres JS. 2008. Two ways to survive infection: what resistance and tolerance can teach us about treating infectious diseases. *Nature Reviews Immunology* **8**:889–895.

Scully EP, Haverfield J, Ursin RL, Tannenbaum C, Klein SL. 2020. Considering how biological sex impacts immune responses and COVID-19 outcomes. *Nat Rev Immunol* **20**:442–447.

Solana R, Tarazona R, Gayoso I, Lesur O, Dupuis G, Fulop T. 2012. Innate immunosenescence: effect of aging on cells and receptors of the innate immune system in humans. *Semin Immunol* **24**:331–341.

Tesoriero JM, Swain C-AE, Pierce JL, Zamboni L, Wu M, Holtgrave DR, Gonzalez CJ, Udo T, Morne JE, Hart-Malloy R, Rajulu DT, Leung S-YJ, Rosenberg ES. 2021. COVID-19 Outcomes Among Persons Living With or Without Diagnosed HIV Infection in New York State. *JAMA Netw Open* **4**:e2037069.

Verdoni L, Mazza A, Gervasoni A, Martelli L, Ruggeri M, Ciuffreda M, Bonanomi E, D'Antiga L. 2020. An outbreak of severe Kawasaki-like disease at the Italian epicentre of the SARS-CoV-2 epidemic: an observational cohort study. *Lancet* **395**:1771–1778.

Vivier E, Artis D, Colonna M, Diefenbach A, Di Santo JP, Eberl G, Koyasu S, Locksley RM, McKenzie ANJ, Mebius RE, Powrie F, Spits H. 2018. Innate Lymphoid Cells: 10 Years On. *Cell* **174**:1054–1066.

1140 Wang A, Huen SC, Luan HH, Yu S, Zhang C, Gallezot J-D, Booth CJ, Medzhitov R. 2016.
1141 Opposing Effects of Fasting Metabolism on Tissue Tolerance in Bacterial and Viral
1142 Inflammation. *Cell* **166**:1512-1525.e12.
1143 Wang Y, Lifshitz L, Gellatly K, Vinton CL, Busman-Sahay K, McCauley S, Vangala P, Kim
1144 K, Derr A, Jaiswal S, Kucukural A, McDonel P, Hunt PW, Greenough T, Houghton
1145 J, Somsouk M, Estes JD, Brenchley JM, Garber M, Deeks SG, Luban J. 2020.
1146 HIV-1-induced cytokines deplete homeostatic innate lymphoid cells and expand
1147 TCF7-dependent memory NK cells. *Nat Immunol* **21**:274–286.
1148 Whittaker E, Bamford A, Kenny J, Kaforou M, Jones CE, Shah P, Ramnarayan P, Fraisse
1149 A, Miller O, Davies P, Kucera F, Brierley J, McDougall M, Carter M, Tremoulet A,
1150 Shimizu C, Herberg J, Burns JC, Lyall H, Levin M, PIMS-TS Study Group and
1151 EUCLIDS and PERFORM Consortia. 2020. Clinical Characteristics of 58 Children
1152 With a Pediatric Inflammatory Multisystem Syndrome Temporally Associated With
1153 SARS-CoV-2. *JAMA* **324**:259–269.
1154 Wickham H. 2016. ggplot2: Elegant Graphics for Data Analysis. Springer.
1155 Wickham H, Averick M, Bryan J, Chang W, McGowan L, François R, Grolemund G, Hayes
1156 A, Henry L, Hester J, Kuhn M, Pedersen T, Miller E, Bache S, Müller K, Ooms J,
1157 Robinson D, Seidel D, Spinu V, Takahashi K, Vaughan D, Wilke C, Woo K, Yutani
1158 H. 2019. Welcome to the Tidyverse. *JOSS* **4**:1686.
1159 Yang Q, Monticelli LA, Saenz SA, Chi AW-S, Sonnenberg GF, Tang J, De Obaldia ME,
1160 Bailis W, Bryson JL, Toscano K, Huang J, Haczku A, Pear WS, Artis D, Bhandoola
1161 A. 2013. T cell factor 1 is required for group 2 innate lymphoid cell generation.
1162 *Immunity* **38**:694–704.

1163 Yang Q, Saldi TK, Gonzales PK, Lasda E, Decker CJ, Tat KL, Fink MR, Hager CR, Davis
1164 JC, Ozeroff CD, Muhlrad D, Clark SK, Fattor WT, Meyerson NR, Paige CL,
1165 Gilchrist AR, Barbachano-Guerrero A, Worden-Sapper ER, Wu SS, Brisson GR,
1166 McQueen MB, Dowell RD, Leinwand L, Parker R, Sawyer SL. 2021. Just 2% of
1167 SARS-CoV-2−positive individuals carry 90% of the virus circulating in
1168 communities. *Proc Natl Acad Sci U S A* **118**. doi:10.1073/pnas.2104547118
1169 Yonker LM, Gilboa T, Ogata AF, Senussi Y, Lazarovits R, Boribong BP, Bartsch YC,
1170 Loiselle M, Noval Rivas M, Porritt RA, Lima R, Davis JP, Farkas EJ, Burns MD,
1171 Young N, Mahajan VS, Hajizadeh S, Herrera Lopez XI, Kreuzer J, Morris R,
1172 Martinez EE, Han I, Griswold K Jr, Barry NC, Thompson DB, Church G, Edlow AG,
1173 Haas W, Pillai S, Arditi M, Alter G, Walt DR, Fasano A. 2021. Multisystem
1174 inflammatory syndrome in children is driven by zonulin-dependent loss of gut
1175 mucosal barrier. *J Clin Invest*. doi:10.1172/JCI149633
1176 Yonker LM, Neilan AM, Bartsch Y, Patel AB, Regan J, Arya P, Gootkind E, Park G,
1177 Hardcastle M, St John A, Appleman L, Chiu ML, Fialkowski A, De la Flor D, Lima
1178 R, Bordt EA, Yockey LJ, D'Avino P, Fischinger S, Shui JE, Lerou PH, Bonventre
1179 JV, Yu XG, Ryan ET, Bassett IV, Irimia D, Edlow AG, Alter G, Li JZ, Fasano A.
1180 2020. Pediatric Severe Acute Respiratory Syndrome Coronavirus 2 (SARS-CoV-
1181 2): Clinical Presentation, Infectivity, and Immune Responses. *J Pediatr* **227**:45-
1182 52.e5.
1183 Yu G, Wang L-G, Han Y, He Q-Y. 2012. clusterProfiler: an R Package for Comparing
1184 Biological Themes Among Gene Clusters. *OMICS* **16**:284–287.

1185 Yudanin NA, Schmitz F, Flamar A-L, Thome JJC, Tait Wojno E, Moeller JB, Schirmer M,
1186 Latorre IJ, Xavier RJ, Farber DL, Monticelli LA, Artis D. 2019. Spatial and Temporal
1187 Mapping of Human Innate Lymphoid Cells Reveals Elements of Tissue Specificity.
1188 *Immunity* **50**:505-519.e4.
1189 Yukselen O, Turkyilmaz O, Ozturk AR, Garber M, Kucukural A. 2020. DolphinNext: a
1190 distributed data processing platform for high throughput genomics. *BMC*
1191 *Genomics* **21**:310.
1192 Zhang Z-L, Hou Y-L, Li D-T, Li F-Z. 2020. Laboratory findings of COVID-19: a systematic
1193 review and meta-analysis. *Scand J Clin Lab Invest* **80**:441–447.
1194 Zhao Q, Meng M, Kumar R, Wu Y, Huang J, Deng Y, Weng Z, Yang L. 2020.
1195 Lymphopenia is associated with severe coronavirus disease 2019 (COVID-19)
1196 infections: A systemic review and meta-analysis. *Int J Infect Dis* **96**:131–135.
1197 Zheng M, Gao Y, Wang G, Song G, Liu S, Sun D, Xu Y, Tian Z. 2020. Functional
1198 exhaustion of antiviral lymphocytes in COVID-19 patients. *Cell Mol Immunol*.
1199 Zhou F, Yu T, Du R, Fan G, Liu Y, Liu Z, Xiang J, Wang Y, Song B, Gu X, Guan L, Wei
1200 Y, Li H, Wu X, Xu J, Tu S, Zhang Y, Chen H, Cao B. 2020. Clinical course and risk
1201 factors for mortality of adult inpatients with COVID-19 in Wuhan, China: a
1202 retrospective cohort study. *Lancet* **395**:1054–1062.
1203
1204
1205
1206
1207

ACKNOWLEDGEMENTS

We thank the Massachusetts Consortium for Pathogen Readiness Specimen Collection and Processing Team listed below and members of the Yu and Luban Labs. This work was supported in part by the Massachusetts Consortium for Pathogen Readiness through grants from the Evergrande Fund and NIH grants R37AI147868 and R01AI148784 to J.L. and Ruth L. Kirschstein NRSA Fellowship F30HD100110 to N.J.S. The MGH/MassCPR COVID biorepository was supported by a gift from Ms. Enid Schwartz, by the Mark and Lisa Schwartz Foundation, the Massachusetts Consortium for Pathogen Readiness, and the Ragon Institute of MGH, MIT and Harvard. The Pediatric COVID-19 Biorepository was supported by the National Heart, Lung, and Blood Institute (5K08HL143183 to LMY), and the Department of Pediatrics at Massachusetts General Hospital *for* Children (to LMY).

MGH COVID-19 Collection & Processing Team participants Collection Team:
Kendall Lavin-Parsons[1], Blair Parry[1], Brendan Lilley[1], Carl Lodenstein[1], Brenna McKaig[1], Nicole Charland[1], Hargun Khanna[1], Justin Margolin[1]
Processing Team: Anna Gonye[2], Irena Gushterova[2], Tom Lasalle[2], Nihaarika Sharma[2], Brian C. Russo[3], Maricarmen Rojas-Lopez[3], Moshe Sade-Feldman[4], Kasidet Manakongtreecheep[4], Jessica Tantivit[4], Molly Fisher Thomas[4]
Massachusetts Consortium on Pathogen Readiness: Betelihem A. Abayneh[5], Patrick Allen[5], Diane Antille[5], Katrina Armstrong[5], Siobhan Boyce[5], Joan Braley[5], Karen Branch[5], Katherine Broderick[5], Julia Carney[5], Andrew Chan[5], Susan Davidson[5], Michael Dougan[5], David Drew[5], Ashley Elliman[5], Keith Flaherty[5], Jeanne Flannery[5], Pamela Forde[5], Elise Gettings[5], Amanda Griffin[5], Sheila Grimmel[5], Kathleen Grinke[5], Kathryn Hall[5], Meg

Healy[5], Deborah Henault[5], Grace Holland[5], Chantal Kayitesi[5], Vlasta LaValle[5], Yuting Lu[5], Sarah Luthern[5], Jordan Marchewka (Schneider)[5], Brittani Martino[5], Roseann McNamara[5], Christian Nambu[5], Susan Nelson[5], Marjorie Noone[5], Christine Ommerborn[5], Lois Chris Pacheco[5], Nicole Phan[5], Falisha A. Porto[5], Edward Ryan[5], Kathleen Selleck[5], Sue Slaughenhaupt[5], Kimberly Smith Sheppard[5], Elizabeth Suschana[5], Vivine Wilson[5], Galit Alter[6], Alejandro Balazs[6], Julia Bals[6], Max Barbash[6], Yannic Bartsch[6], Julie Boucau[6], Josh Chevalier[6], Fatema Chowdhury[6], Kevin Einkauf[6], Jon Fallon[6], Liz Fedirko[6], Kelsey Finn[6], Pilar Garcia-Broncano[6], Ciputra Hartana[6], Chenyang Jiang[6], Paulina Kaplonek[6], Marshall Karpell[6], Evan C. Lam[6], Kristina Lefteri[6], Xiaodong Lian[6], Mathias Lichterfeld[6], Daniel Lingwood[6], Hang Liu[6], Jinqing Liu[6], Natasha Ly[6], Ashlin Michell[6], Ilan Millstrom[6], Noah Miranda[6], Claire O'Callaghan[6], Matthew Osborn[6], Shiv Pillai[6], Yelizaveta Rassadkina[6], Alexandra Reissis[6], Francis Ruzicka[6], Kyra Seiger[6], Libera Sessa[6], Christianne Sharr[6], Sally Shin[6], Nishant Singh[6], Weiwei Sun[6], Xiaoming Sun[6], Hannah Ticheli[6], Alicja Trocha-Piechocka[6], Daniel Worrall[6], Alex Zhu[6], George Daley[7], David Golan[7], Howard Heller[7], Arlene Sharpe[7], Nikolaus Jilg[8], Alex Rosenthal[8], Colline Wong[8]

[1]Department of Emergency Medicine, Massachusetts General Hospital, Boston, MA, USA.

[2]Massachusetts General Hospital Cancer Center, Boston, MA, USA.

[3]Division of Infectious Diseases, Department of Medicine, Massachusetts General Hospital, Boston, MA, USA.

[4]Massachusetts General Hospital Center for Immunology and Inflammatory Diseases, Boston, MA, USA.

[5]Massachusetts General Hospital, Boston, MA, USA.

[6]Ragon Institute of MGH, MIT and Harvard, Cambridge, MA, USA.

[7]Harvard Medical School, Boston, MA, USA.

[8]Brigham and Women's Hospital, Boston, MA, USA.

Author information

Correspondence and requests for materials should be addressed to J.L. (jeremy.luban@umassmed.edu).